[redacted]FIED

Declassified by authority of NASA
Classification Change Notices No. 113
Dated ** 6/28/67

AERODYNAMIC CHARACTERISTICS OF A TAILLESS FIXED-WING SUPERSONIC TRANSPORT MODEL AT MACH NUMBERS FROM 1.80 TO 2.86

By William A. Corlett and Gerald V. Foster

Langley Research Center
Langley Station, Hampton, Va.

[redacted] 4
[redacted] intervals;
[redacted]ssified after [redacted]

[redacted]SIFIED DOCUMENT—TITLE UNC[redacted]
This mate[redacted] infor[redacted]cting the national defense of [redacted] States within the meaning of the [redacted]ge laws, [redacted] 18, U.S.C., Secs. 793 [redacted], the transmission [redacted]lation of w[redacted]any manner to an unauthorized p[redacted] [redacted]nib. ed by law.

NATIONAL AERONAUTICS AND SPACE ADMINISTRATION

[redacted]

DECLASSIFIED [redacted]

AERODYNAMIC CHARACTERISTICS OF A TAILLESS FIXED-WING

SUPERSONIC TRANSPORT MODEL AT MACH NUMBERS

FROM 1.80 TO 2.86*

By William A. Corlett and Gerald V. Foster
Langley Research Center

SUMMARY

15957

A wind-tunnel investigation has been made through a Mach number range from 1.80 to 2.86 to determine the longitudinal and lateral aerodynamic characteristics of a model of a supersonic transport airplane having three different wing planforms: a modified delta having an ogee-shaped leading edge, a delta, and a trapezoid, both with and without camber and twist.

The results indicated that the trapezoid-wing configuration had the highest maximum lift-drag ratio, although the ogee wing generally provided the lowest values of minimum drag coefficient. Trim control by means of elevon deflection was relatively inefficient and significantly lowered the maximum lift-drag ratio. However, increase in forebody fineness ratio and forebody upsweep had favorable effects on minimum drag and reduced the trim requirements. There was little effect of wing planform on the sideslip parameters for the flat-wing configurations. The cambered and twisted delta- and trapezoid-wing configurations had directional-stability values only slightly less than the flat-wing configurations, whereas the warped ogee wing planform, because of its twist distribution, had the lowest directional-stability level of all the configurations. Conf. Author

INTRODUCTION

The National Aeronautics and Space Administration is currently placing considerable emphasis on configuration studies applicable to supersonic transport aircraft. These studies have been performed on both variable-sweep and fixed-wing configurations throughout a broad Mach number range. (See refs. 1 to 6.) As a part of the fixed-wing study, a tailless configuration has recently been investigated in the Langley 4- by 4-foot supersonic pressure tunnel at a Mach number of 2.20, and the results are reported in reference 7. This configuration has been investigated further in the Langley Unitary Plan wind tunnel from Mach numbers 1.80 to 2.86, and the results are presented herein.

The test configuration consisted of a low-wing—body—vertical-tail combination with removable engine nacelles. Three wing planforms including an ogee,

*Title, Unclassified.

[redacted]

a delta, and a trapezoid were investigated both with and without camber and twist. Two alternate forebodies were also investigated to determine the combined effects of upsweeping the forebody and increasing the fineness ratio, for the twisted and cambered ogee-wing configuration. The tests were performed at a Reynolds number per foot of 2.5×10^6. The angle of attack was varied from about -4° to 12°, and the angle of sideslip was varied from about -4° to 6°.

SYMBOLS

The results are referred to the body-axis system except for the lift and drag coefficients which are referred to the stability-axis system. The moment center for all configurations is located on the model reference line at a point 61.76 percent of the body length behind the basic nose. This location is 2.36 percent of the body length aft of the reference used in reference 7.

α	angle of attack, deg
b	wing span, 19.25 in.
β	angle of sideslip, deg
c	local chord, in.
$\bar{c}$	reference chord, 12.00 in.
C_D	drag coefficient, $\frac{\text{Drag}}{qS}$
$C_{D,B}$	nacelle-base-drag coefficient, $\frac{\text{Nacelle-base-drag}}{qS}$
$C_{D,b}$	balance-chamber-drag coefficient, $\frac{\text{Chamber drag}}{qS}$
$C_{D,i}$	nacelle-internal-drag coefficient, $\frac{\text{Nacelle-internal-drag}}{qS}$
C_L	lift coefficient, $\frac{\text{Lift}}{qS}$
C_l	rolling-moment coefficient, $\frac{\text{Rolling moment}}{qSb}$
C_m	pitching-moment coefficient, $\frac{\text{Pitching moment}}{qS\bar{c}}$

$C_{m,o}$ pitching-moment coefficient at $C_L = 0$

C_n yawing-moment coefficient, $\frac{\text{Yawing moment}}{qSb}$

C_Y side-force coefficient, $\frac{\text{Side force}}{qS}$

C_{L_α} lift-curve slope, per deg

C_{l_β} effective-dihedral parameter, $\frac{\Delta C_l}{\Delta\beta}$, per deg

C_{n_β} directional-stability parameter, $\frac{\Delta C_n}{\Delta\beta}$, per deg

C_{Y_β} side-force parameter, $\frac{\Delta C_Y}{\Delta\beta}$, per deg

L/D lift-drag ratio

$\frac{\partial C_m}{\partial C_L}$ longitudinal-stability parameter

M Mach number

δ_e elevon deflection angle, deg

q free-stream dynamic pressure, lb/sq ft

S reference area of wing including body intercept, 1.665 sq ft

x,y,z Cartesian coordinate system with origin at leading edge of wing root

Subscripts:

max maximum

min minimum

MODEL

Dimensional details of the model are shown in a drawing presented as figure 1, and the geometric characteristics are presented in table I. The model incorporated planar wings having three different interchangeable planforms that consisted of a modified delta having an S-shaped leading edge (referred to as the ogee wing), a delta, and a trapezoid. In addition, three wings utilizing the same planforms were designed to incorporate a camber and twist distribution for a lift coefficient of 0.10 at a Mach number of 2.20. A sketch showing a comparison of the three wing planforms is presented as figure 2.

The wing-design lift coefficient has been used herein to identify the planar $\left(C_{L,design} = 0\right)$, and the cambered and twisted wings $\left(C_{L,design} = 0.10\right)$. The warped ogee wing used herein includes a leading-edge camber modification (ref. 7) over the outer 35 percent of the semispan. The wings have a streamwise thickness-chord ratio of 0.03 at the root and 0.02 at the tip with an essentially linear variation between these points. The camber and twist distributions for the warped wings are presented in figure 3.

The model was provided with removable engine nacelles which had a constant, straight-line, internal cross section (fig. 1(e)). The flat wing planforms were equipped with trailing-edge elevons located inboard and outboard of the nacelles. The model was also provided with two alternate forebodies, designated herein as F_2 and F_3, which had progressively more upsweep and an effective fineness ratio of 5.7 as compared with a fineness ratio of 4.7 for the basic forebody, F_1. (See fig. 1(d).) Photographs of the model with the ogee wing and basic forebody $\left(F_1\right)$ are presented in figure 4.

TESTS, CORRECTIONS, AND ACCURACY

The tests were conducted in the low Mach number test section of the Langley Unitary Plan wind tunnel, which is a continuous-flow, variable-pressure facility. The test section is about 4- by 4-feet square and is about 7 feet in length. The nozzle leading to the test section is of the asymmetric sliding-block type which permits variation in Mach number from 1.47 to 2.86 without tunnel shutdown.

Tests were performed on the three different wing planforms, with and without camber and twist, with the engine nacelles removed. In addition, engine nacelles and plain flap-type trailing-edge elevons with a deflection of -10° were tested on the flat ogee wing planform.

Forces and moments on the model were measured by means of a six-component, electrical strain-gage balance mounted within the model fuselage. Tests were made through an angle-of-attack range from approximately -4° to 12° and through a range of sideslip angle from approximately -4° to 6°. The angles of attack and sideslip have been corrected for deflection of balance and sting due to the aerodynamic loads. The balance-chamber pressure and nacelle base pressures were measured, and the drag forces were adjusted to correspond to free-stream static pressure acting over the model chamber and nacelle bases. The drag-force results were also corrected for the internal skin-friction drag and the drag component of the normal force produced by the air which passes through the nacelle ducts. These corrections are presented in figure 5.

The tests were made at a constant Reynolds number per foot of 2.5×10^{6}. The stagnation dewpoint was maintained low enough (-25° F or less) to prevent condensation effects. Other test conditions are shown in the following table:

Mach number	Stagnation temperature, °F	Stagnation pressure, lb/sq ft
1.80	150	1590
2.20	150	1820
2.86	150	2560

In order to provide a turbulent boundary layer, 1/16-inch-wide strips of No. 60 carborundum grains (approximate diameter of 0.012 inch) were placed on the wings and vertical tail 3/16 inch normal to the leading edge and 1 inch behind the fuselage nose.

Based on balance calibration and data repeatability, the data presented herein are estimated to be accurate within the following limits:

C_L . . . . ±0.0038
C_D . . . . ±0.0006
C_m . . . . ±0.0022
C_l . . . . ±0.0008
C_n . . . . ±0.0012
C_Y . . . . ±0.0016
M . . . . ±0.015
α, deg . . . . ±0.1
β, deg . . . . ±0.1

RESULTS AND DISCUSSION

Longitudinal Characteristics

The effects of wing planform on the longitudinal aerodynamic characteristics of the flat- and the warped-wing configurations (nacelles off) are presented in figures 6 and 7, respectively, for Mach numbers of 1.80 and 2.86. The variation of the aerodynamic characteristics with change in Mach number is shown in figure 8. This figure presents data obtained for a Mach number of 2.20 which was reported on in reference 7 as well as the data obtained in the present investigation for $M = 1.80$ and $M = 2.86$. The lift and pitching-moment-coefficient curves for all of the wing configurations with the basic forebody (F_1) are relatively linear in the test Mach number range, and all of the configurations produce the familiar decrease in lift-curve slope and static margin with increase in Mach number. Although the ogee-wing configuration generally provided the lowest values of minimum drag coefficient, the trapezoid-wing configuration had the highest maximum lift-drag ratio because of a lower value of drag due to lift for this wing. For all three wing planforms, the use of camber and twist provided an increase in $(L/D)_{max}$ at Mach numbers of 1.80 and 2.20 but had little effect on $(L/D)_{max}$ at a Mach number of 2.86. The maximum, untrimmed, lift-drag ratio for the warped-trapezoid-wing configuration varies from about 7.2 at Mach number 1.80 to about 6.1 at Mach number 2.86 as compared with a lift-drag-ratio variation of 6.7 to 6.1 for the flat-trapezoid-wing configuration.

The effects of elevon deflection on the aerodynamic characteristics in pitch are presented in figure 9 for the flat-ogee-wing configuration. These data show that a 10° elevon setting will not trim the configuration to the C_L for $(L/D)_{max}$ at either Mach number tested with the moment center used. Further, if the static margin were reduced to provide trim at $(L/D)_{max}$ with a 10° elevon deflection, the decrease in performance would be quite severe (a loss of about 1.0 in $(L/D)_{max}$ at Mach number 1.80 and about 0.7 at Mach number 2.86).

The results presented in figure 10 show the combined effects of an increase in forebody length and upsweep on the longitudinal aerodynamic characteristics of the warped-ogee-wing configuration. Both modified forebodies F_2 and F_3 had a favorable effect on $C_{m,o}$ and $C_{D,min}$ at Mach numbers 1.80 and 2.86; however, the stability level of the F_3 configuration decreased significantly at the higher values of lift coefficient.

Sideslip Characteristics

Some basic sideslip data for both the flat- and the warped-ogee-wing configurations at Mach numbers of 1.80 and 2.86 at an angle of attack of 8° are presented in figure 11. These curves are generally representative of the linearity of the sideslip data of all the test configurations. The remainder of the sideslip data presented are in parameter form derived from differences in data obtained from pitch tests at sideslip angles of 0° and approximately 4°.

There is little effect of wing planform on sideslip parameters at the test Mach numbers and angles of attack for the flat-wing configurations. (See fig. 12.) All the configurations (with nacelles off) have a positive effective dihedral which increases with increasing angle of attack. The configurations are directionally stable to an angle of attack of about 12° at Mach number 1.80; however, at Mach number 2.86 directional stability is only maintained to an angle of attack of about 6°. Similar stability characteristics are noted for the warped-delta-wing and warped-trapezoid-wing configurations (see fig. 13), although the directional stability for these two cambered and twisted configurations is slightly less than that of their flat-wing counterparts. There is a reduction in directional stability for the warped-ogee-wing configuration as compared with the configuration with the flat ogee wing at both test Mach numbers. The tail-off results obtained with the warped ogee and trapezoid planforms indicate that the loss in directional stability of the ogee wing is inherent in the wing camber and twist and is not associated with a change in vertical-tail effectiveness.

[redacted]

CONCLUDING REMARKS

The aerodynamic characteristics of a tailless supersonic transport airplane having three different wing planforms (ogee, delta, and trapezoid) both with and without camber and twist have been investigated in the Mach number range from 1.80 to 2.86. The wind-tunnel results indicated that the trapezoid-wing configuration had the highest maximum lift-drag ratio, although the ogee-wing configuration generally provided the lowest values of minimum drag coefficient. Trim control by means of elevon deflection was relatively inefficient and significantly lowered the maximum lift-drag ratio. However, increase in forebody fineness ratio and forebody upsweep had favorable effects on minimum drag and reduced the trim requirements. There was little effect of wing planform on the sideslip parameters for the flat-wing configurations. The cambered and twisted delta- and trapezoid-wing configurations had directional-stability values only slightly less than the flat-wing configurations, although the warped ogee wing planform had a somewhat lower directional-stability level at each test Mach number resulting from the wing twist distribution.

Langley Research Center,
National Aeronautics and Space Administration,
Langley Station, Hampton, Va., May 20, 1964.

[redacted]

REFERENCES

1. Staff of the Langley Research Center: The Supersonic Transport - A Technical Summary. NASA TN D-423, 1960.

2. Spearman, M. Leroy, Driver, Cornelius, and Robins, A. Warner: Aerodynamic Characteristics at Mach Numbers of 2.30, 2.96, and 3.50 of a Supersonic Transport Model With a Blended Wing-Body, Variable-Sweep Auxiliary Wing Panels, and Outboard Tail Surfaces. NASA TM X-803, 1963.

3. Whitcomb, Richard T., Patterson, James C., Jr., and Kelly, Thomas C.: An Investigation of the Subsonic, Transonic, and Supersonic Aerodynamic Characteristics of a Proposed Arrow-Wing Transport Airplane Configuration. NASA TM X-800, 1963.

4. Driver, Cornelius, Spearman, M. Leroy, and Corlett, William A.: Aerodynamic Characteristics at Mach Numbers From 1.61 to 2.86 of a Supersonic Transport Model With a Blended Wing-Body, Variable-Sweep Auxiliary Wing Panels, Outboard Tail Surfaces, and a Design Mach Number of 2.2. NASA TM X-817, 1963.

5. Fletcher, LeRoy S.: Static Stability Characteristics of a Delta-Winged Airplane Configuration With Nacelles, a Trapezoidal Canard and a Drooped Tail at Mach Numbers From 0.70 to 3.52. NASA TM X-780, 1963.

6. Sleeman, William C., Jr., and Robins, A. Warner: Low-Speed Investigation of the Aerodynamic Characteristics of a Variable-Sweep Supersonic Transport Configuration Having a Blended Wing and Body. NASA TM X-619, 1962.

7. Foster, Gerald V., and Corlett, William A.: Aerodynamic Characteristics of a Tailless Fixed-Wing Supersonic Transport Configuration at Mach Number 2.20. NASA TM X-960, 1964.

TABLE I.- GEOMETRIC CHARACTERISTICS OF MODEL

Ogee wing:	
Aspect ratio	1.54
Span, in.	19.25
Area of flat wing, sq in.	239.32
Area of warped wing, sq in.	241.36
Root chord, in.	27.78
Mean aerodynamic chord, in.	16.81
Reference chord, in.	12.00
Delta wing:	
Aspect ratio	1.54
Span, in.	19.25
Area, sq in	239.94
Root chord, in.	24.87
Mean aerodynamic chord, in.	16.56
Reference chord, in.	12.00
Trapezoid wing:	
Aspect ratio	1.54
Span, in.	19.25
Area, sq in.	240.64
Root chord, in.	23.30
Tip chord, in.	1.84
Mean aerodynamic chord, in.	15.46
Reference chord, in.	12.00
Vertical tail:	
Root chord, in.	7.64
Tip chord, in.	2.40
Area, sq in.	21.64
Fuselage:	
Length with basic forebody (F_1), in.	42.50
Length with modified forebodies $(F_2$ and $F_3)$, in.	45.18
Base area, sq in.	2.40
Nacelles:	
Length, in.	10.25
Capture area (each), sq in.	1.04
Base area (each), sq in.	0.96

[redacted]

[redacted]

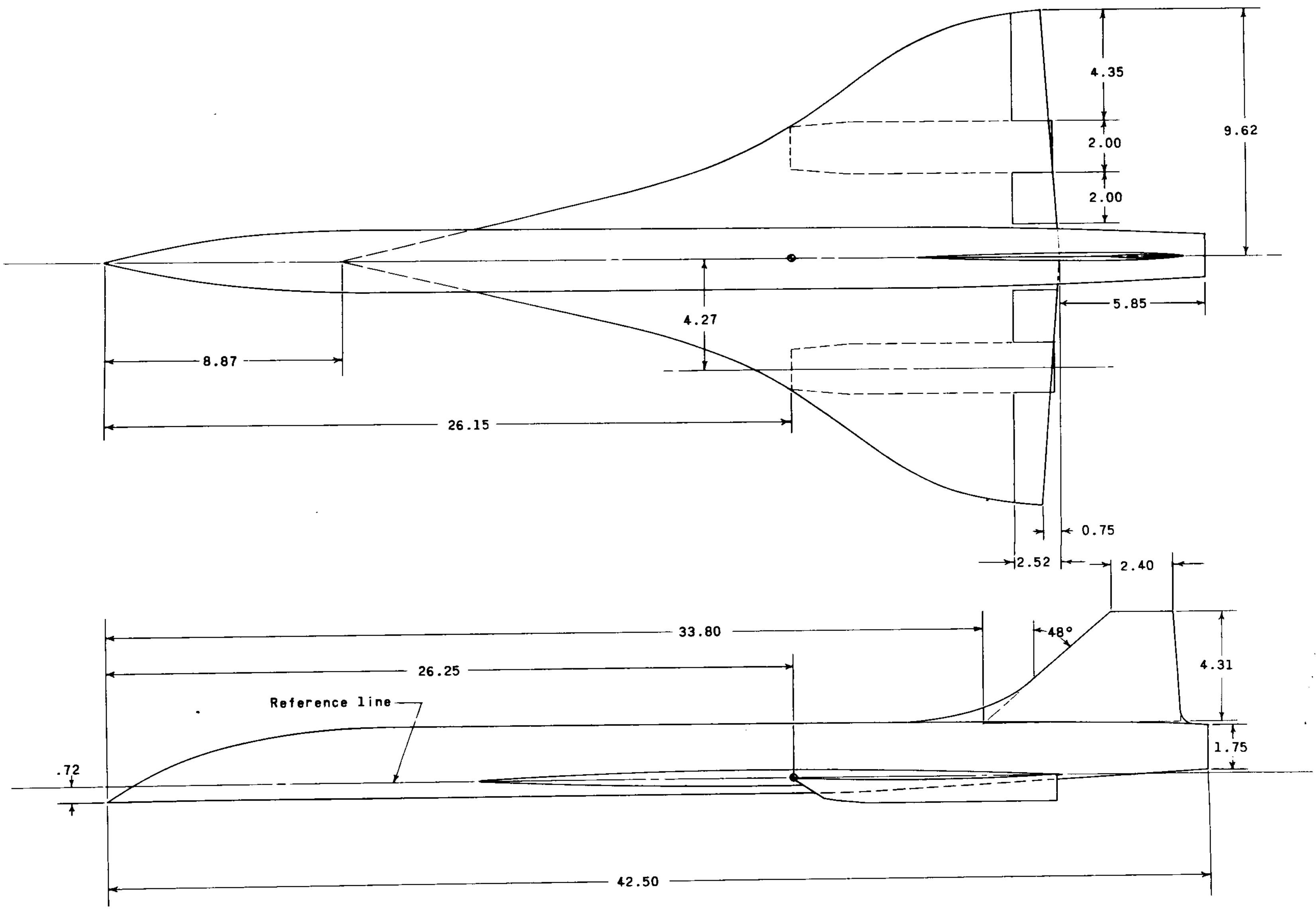

(a) Ogee-wing configuration.

Figure 1.- Details of model. All dimensions in inches.

[redacted]

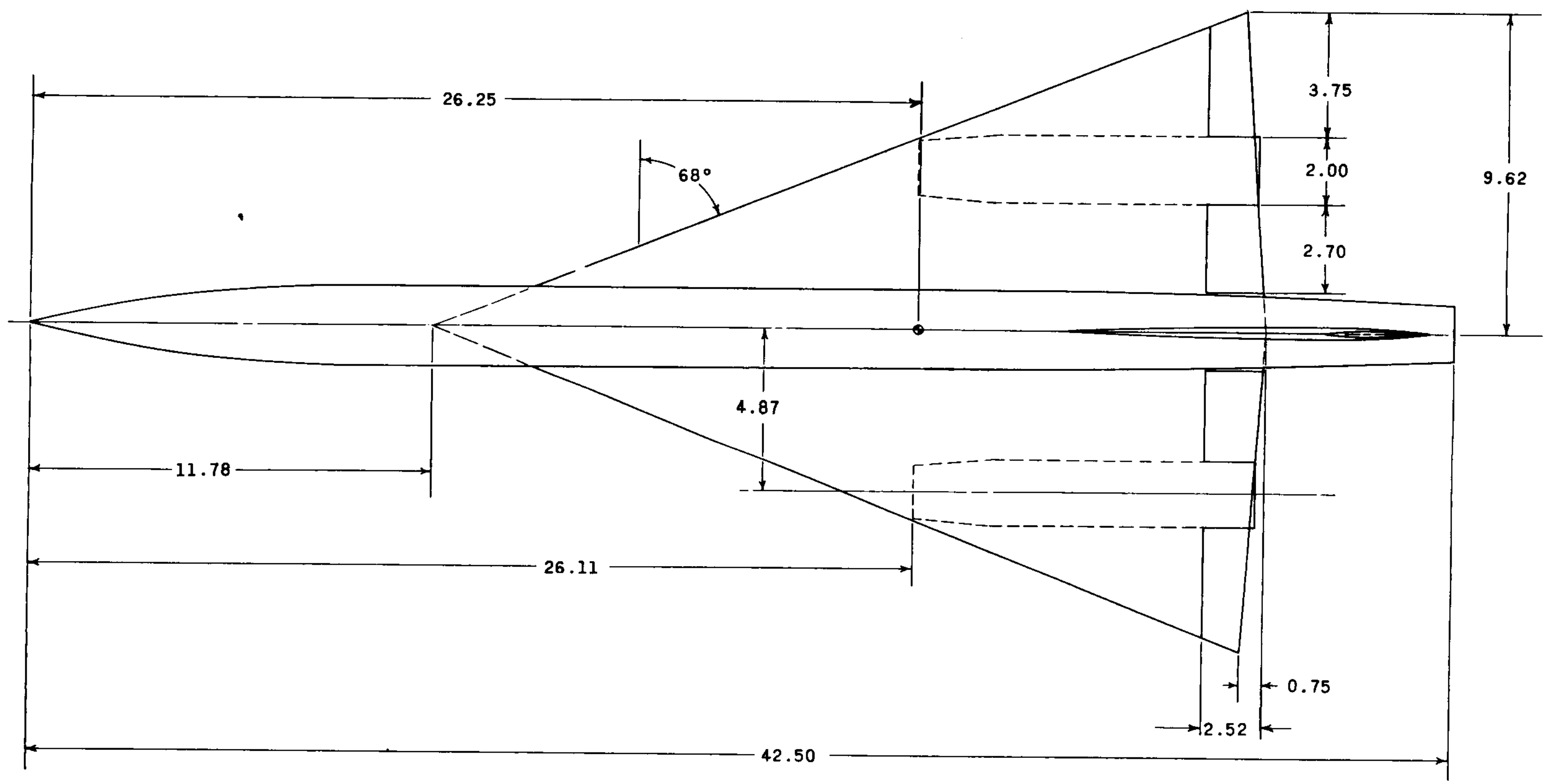

(b) Delta-wing configuration.

Figure 1.- Continued.

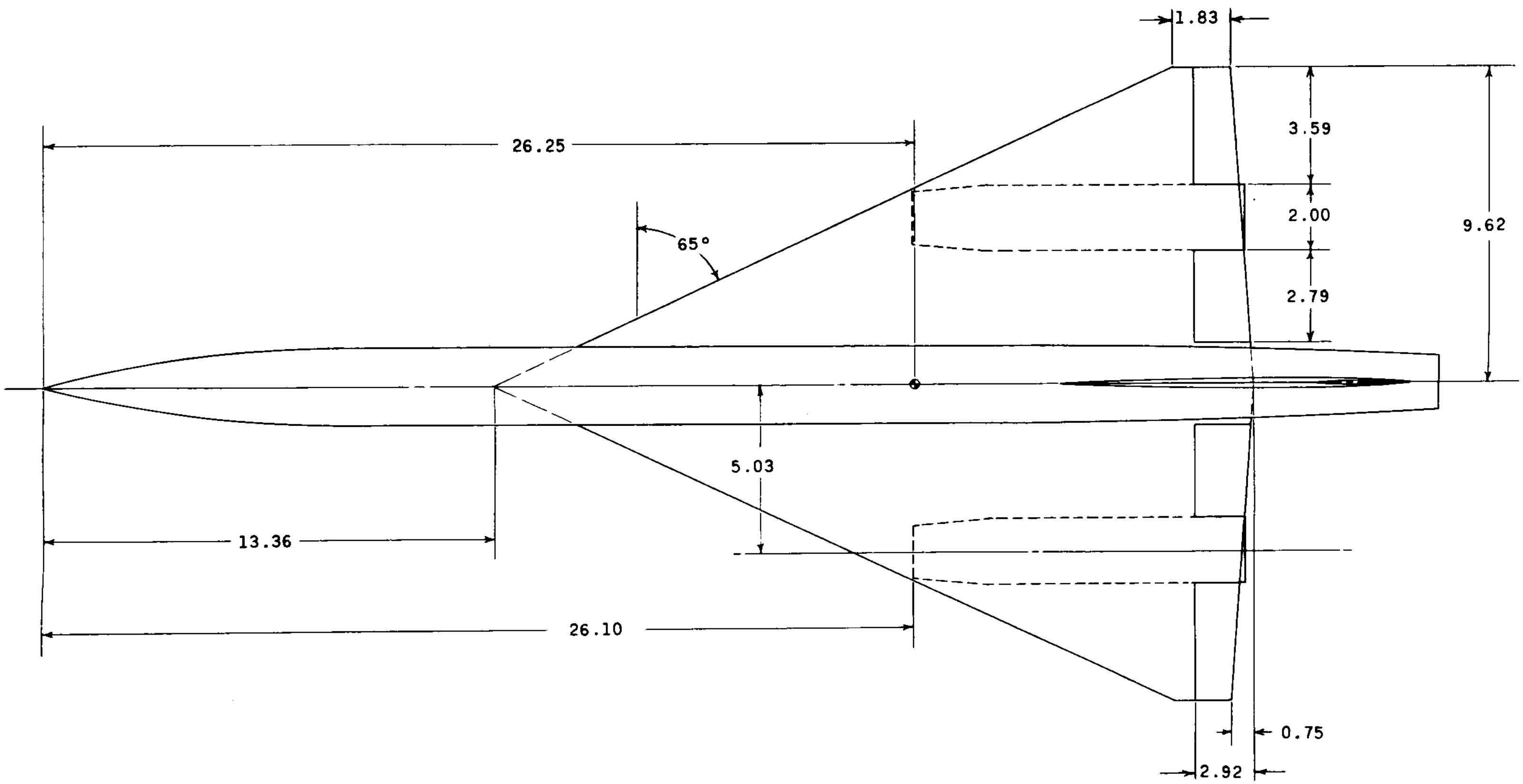

(c) Trapezoid-wing configuration.

Figure 1.- Continued.

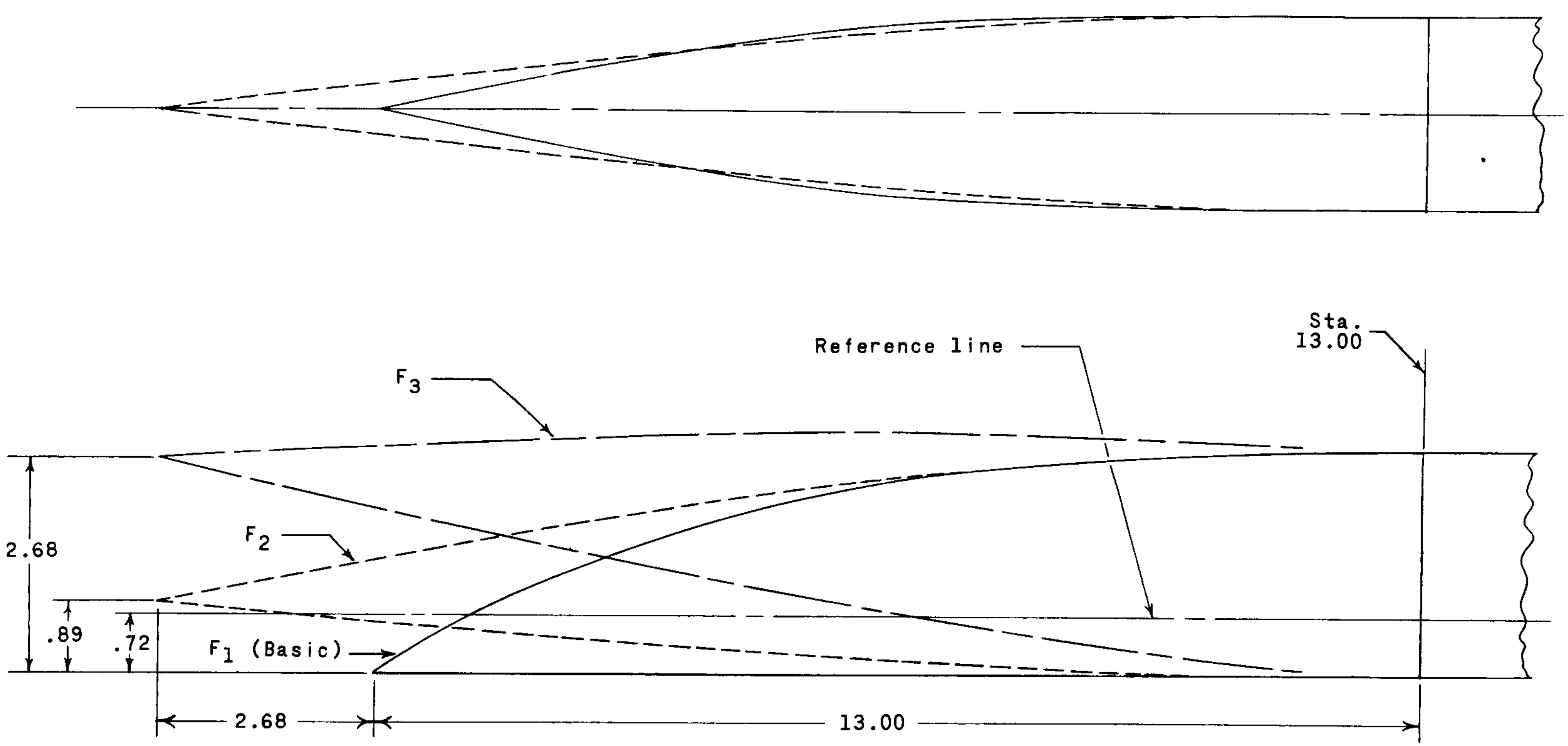

(d) Forebody modifications.

Figure 1.- Continued.

[redacted]

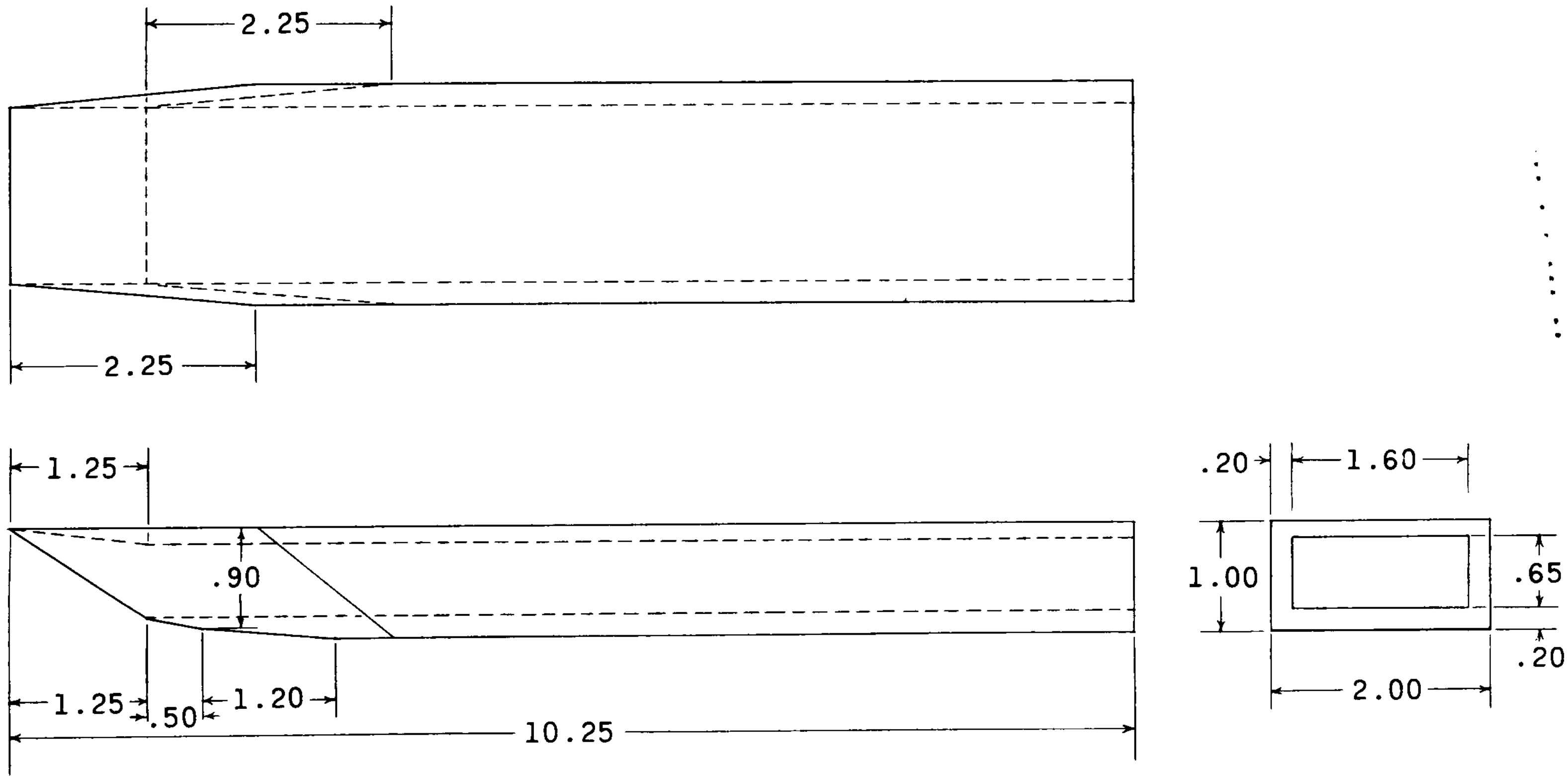

(e) Nacelle.

Figure 1.- Concluded.

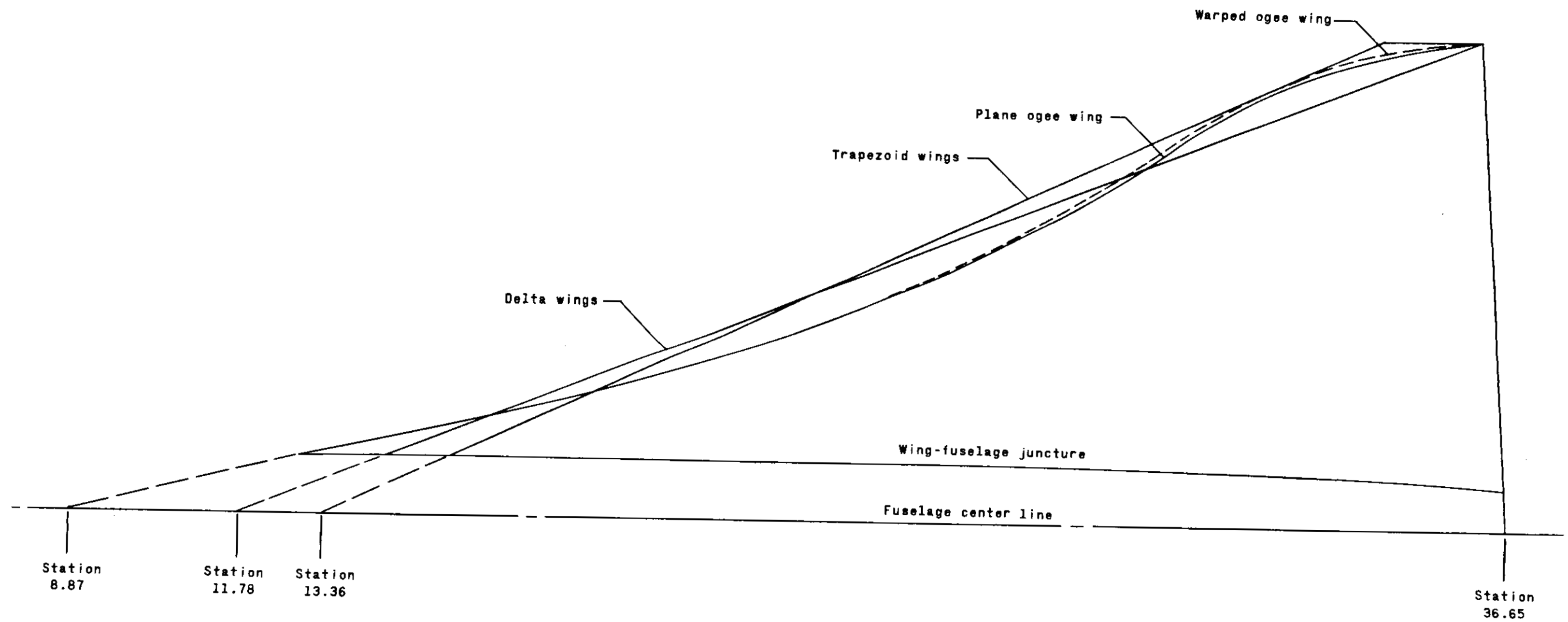

Figure 2.- Comparison of wing planforms.

[redacted]

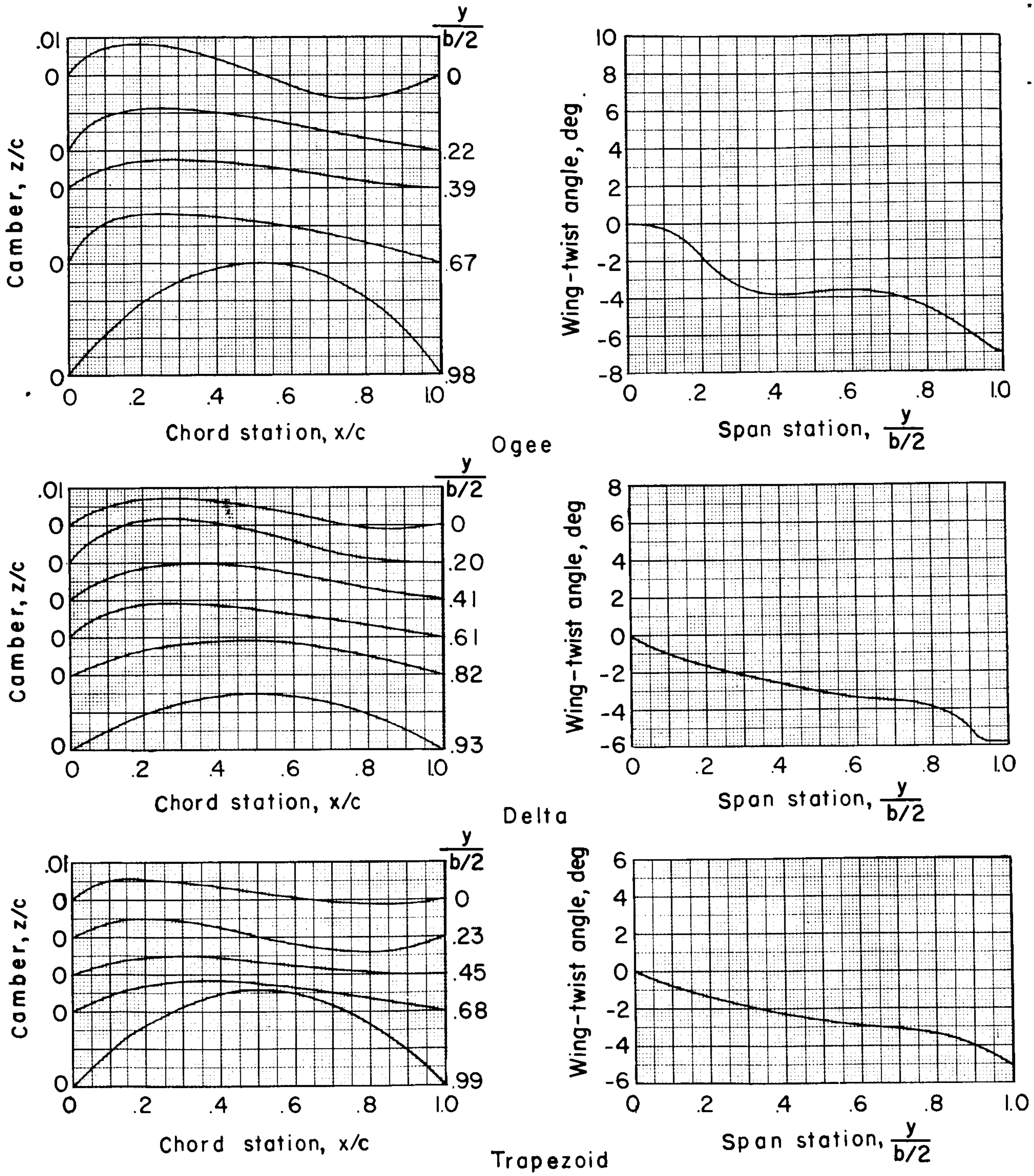

Figure 3.- Variation of camber and twist distribution for ogee, delta, and trapezoid wings.

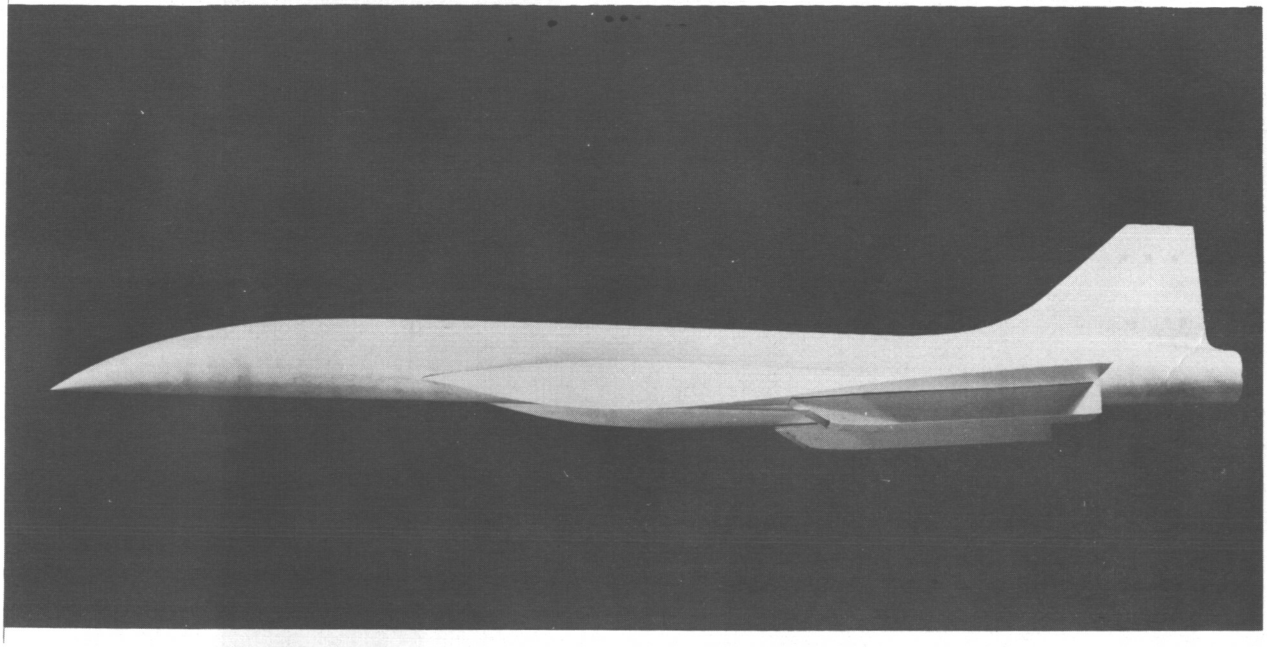

(a) Side view. L-63-10126

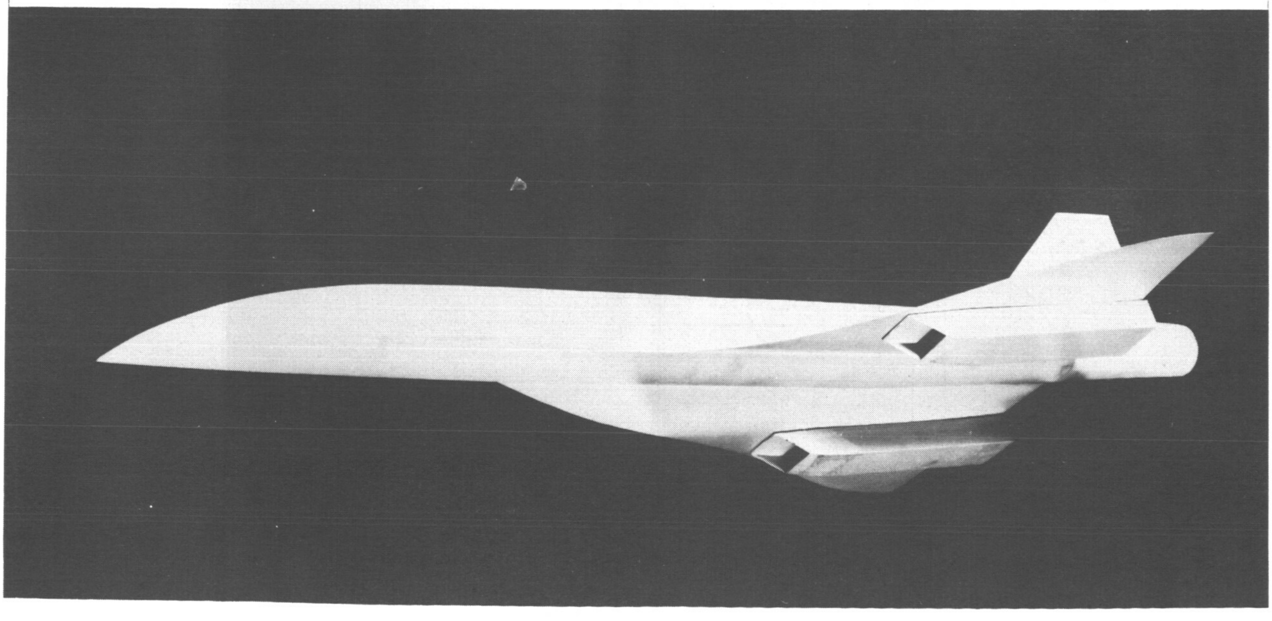

(b) Three-quarter view. L-63-10127

Figure 4.- Photographs of model with ogee wing; $C_{L,design} = 0.10$.

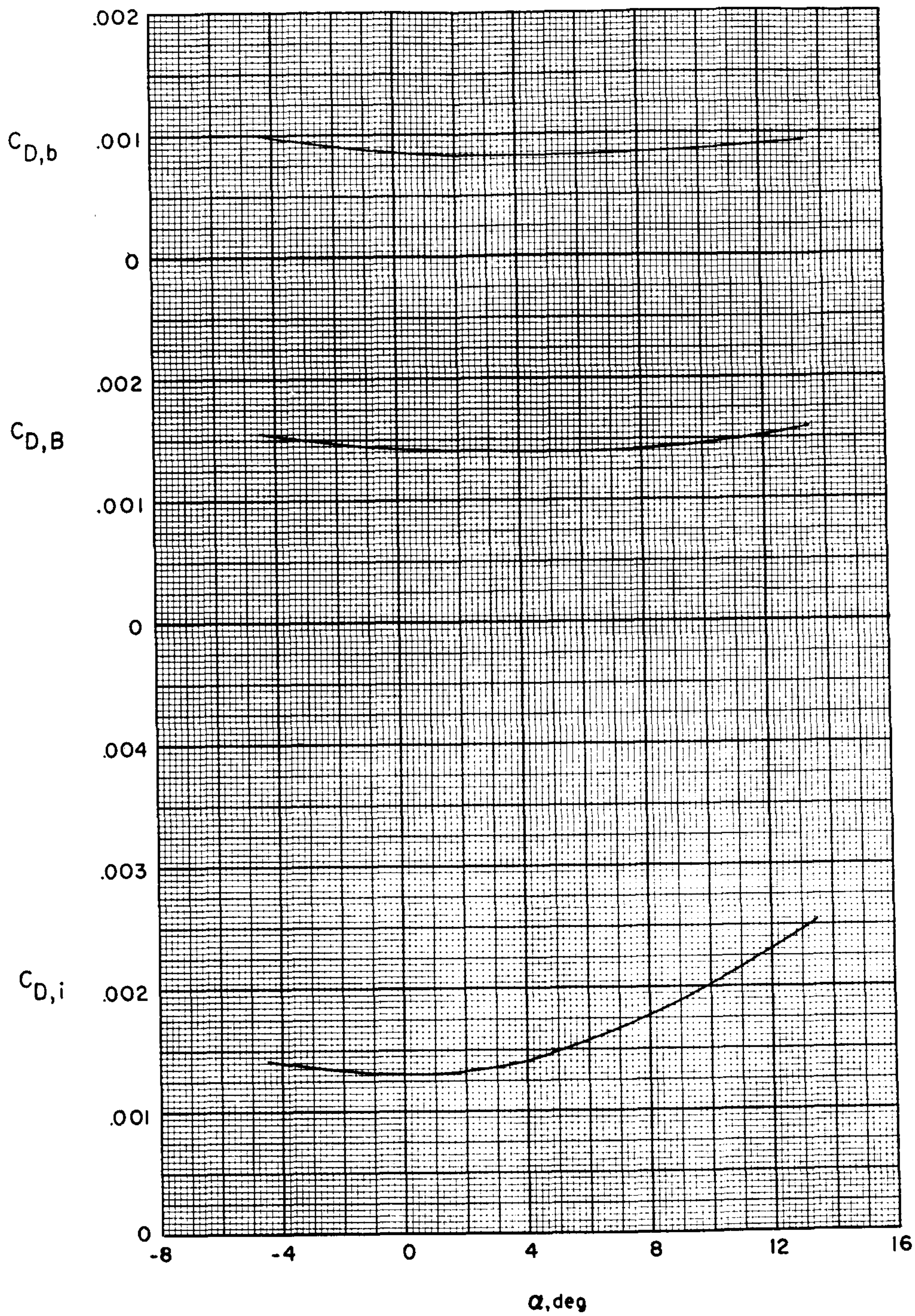

(a) M = 1.80.

Figure 5.- Variation of balance-chamber-drag, nacelle-base-drag, and nacelle-internal-drag coefficients with angle of attack.

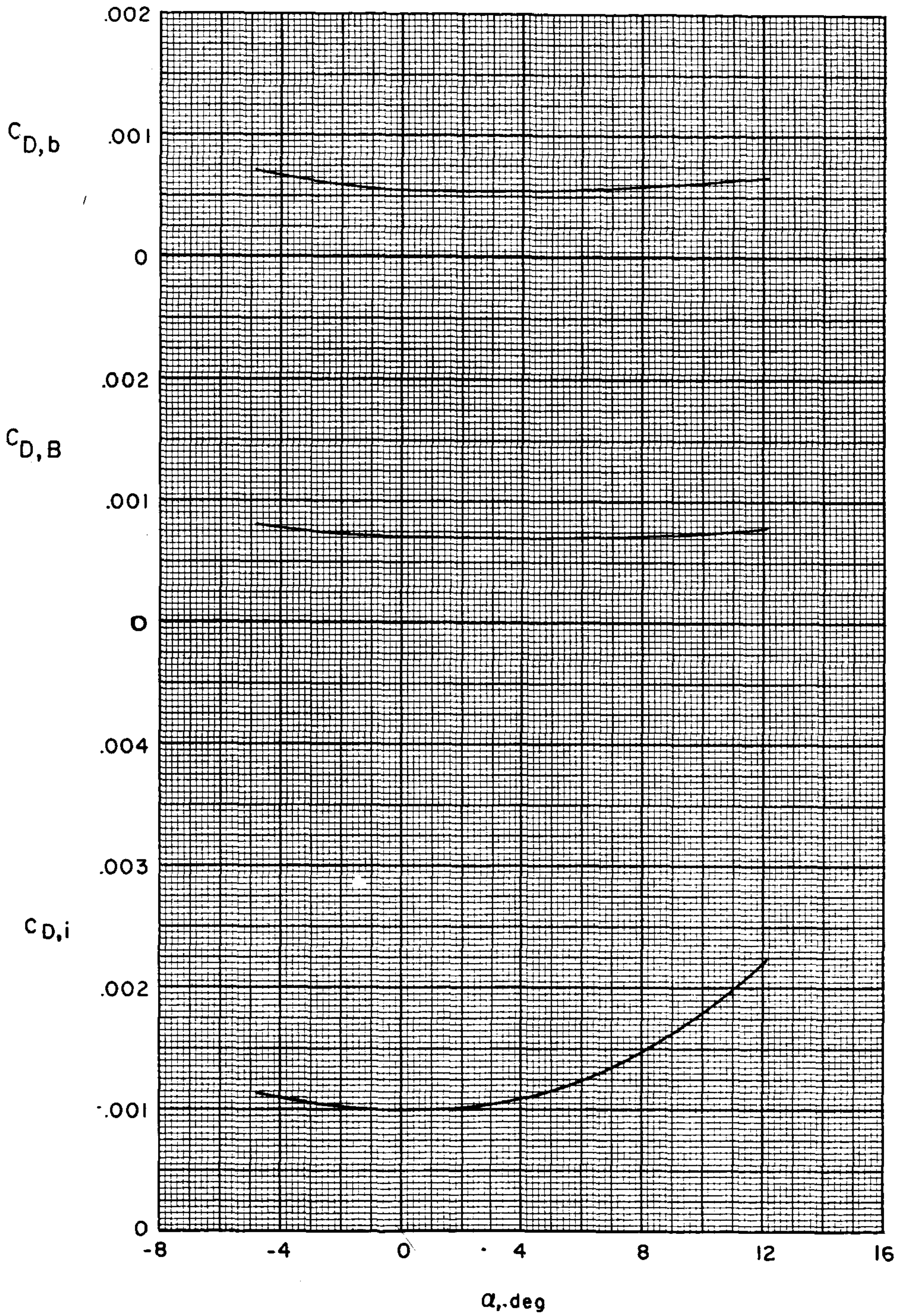

(b) M = 2.86.

Figure 5.- Concluded.

[redacted]

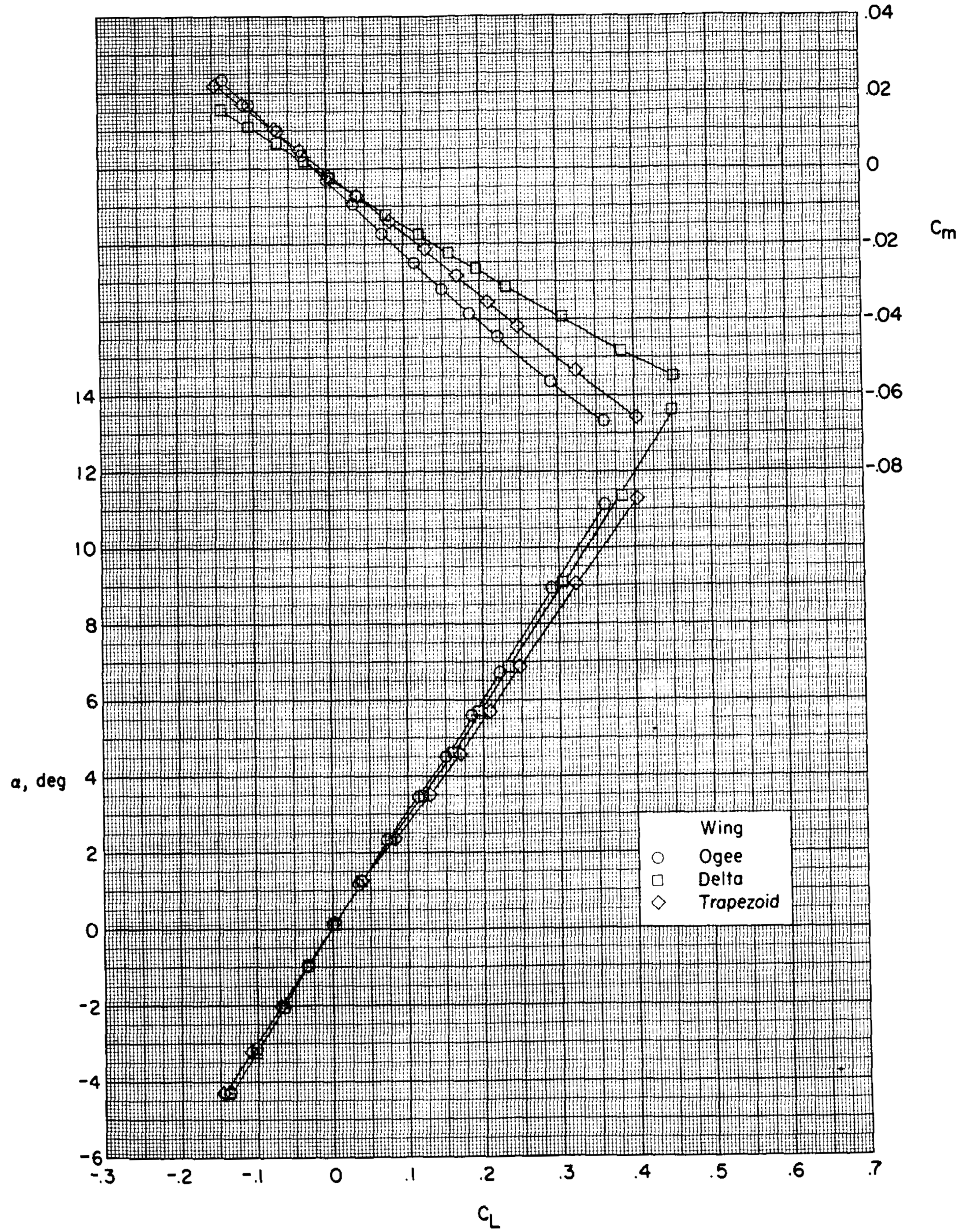

(a) M = 1.80.

Figure 6.- Effect of wing planform on aerodynamic characteristics in pitch. $C_{L,design} = 0$; nacelles off.

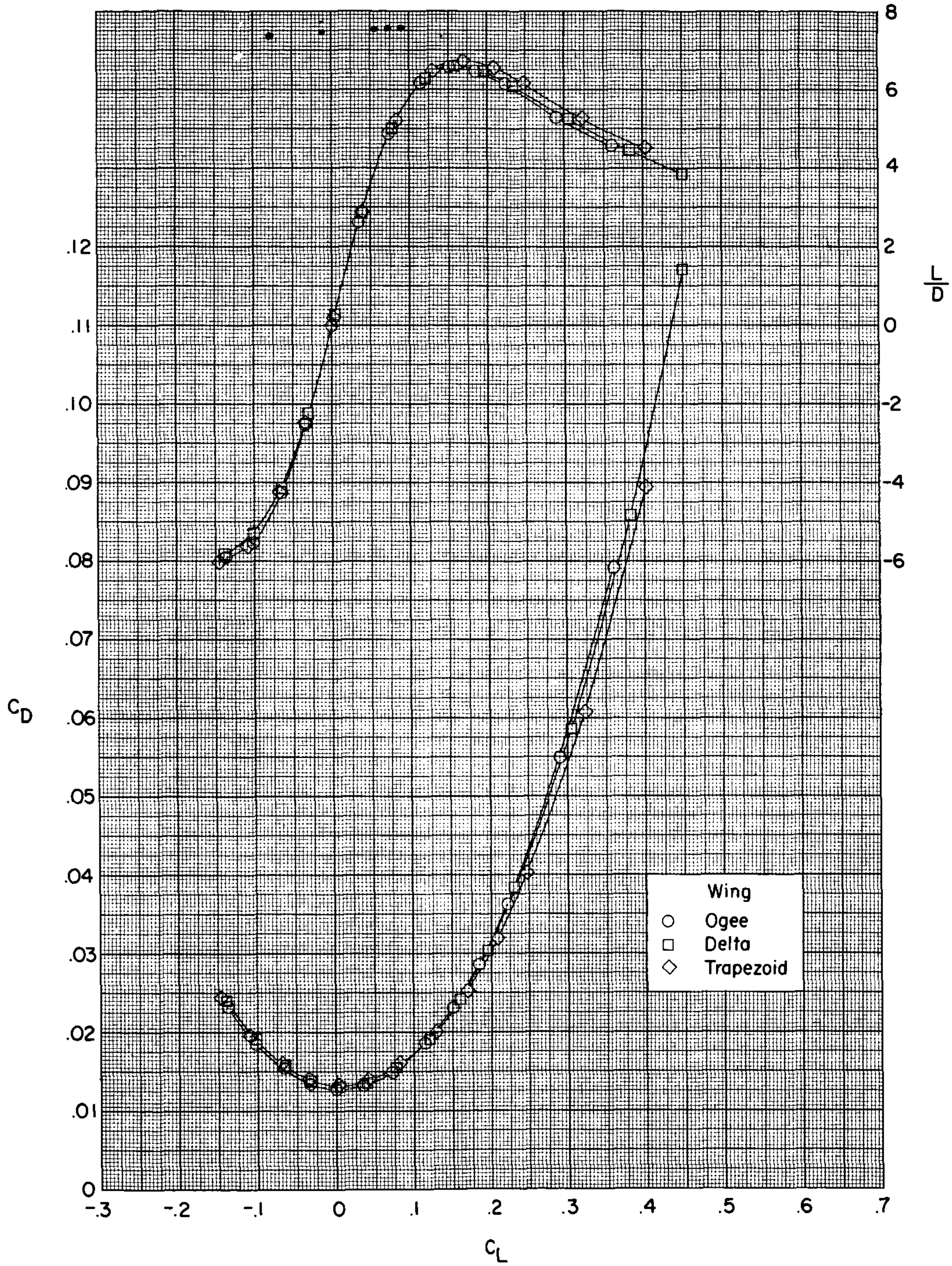

(a) Concluded.

Figure 6.- Continued.

[redacted]

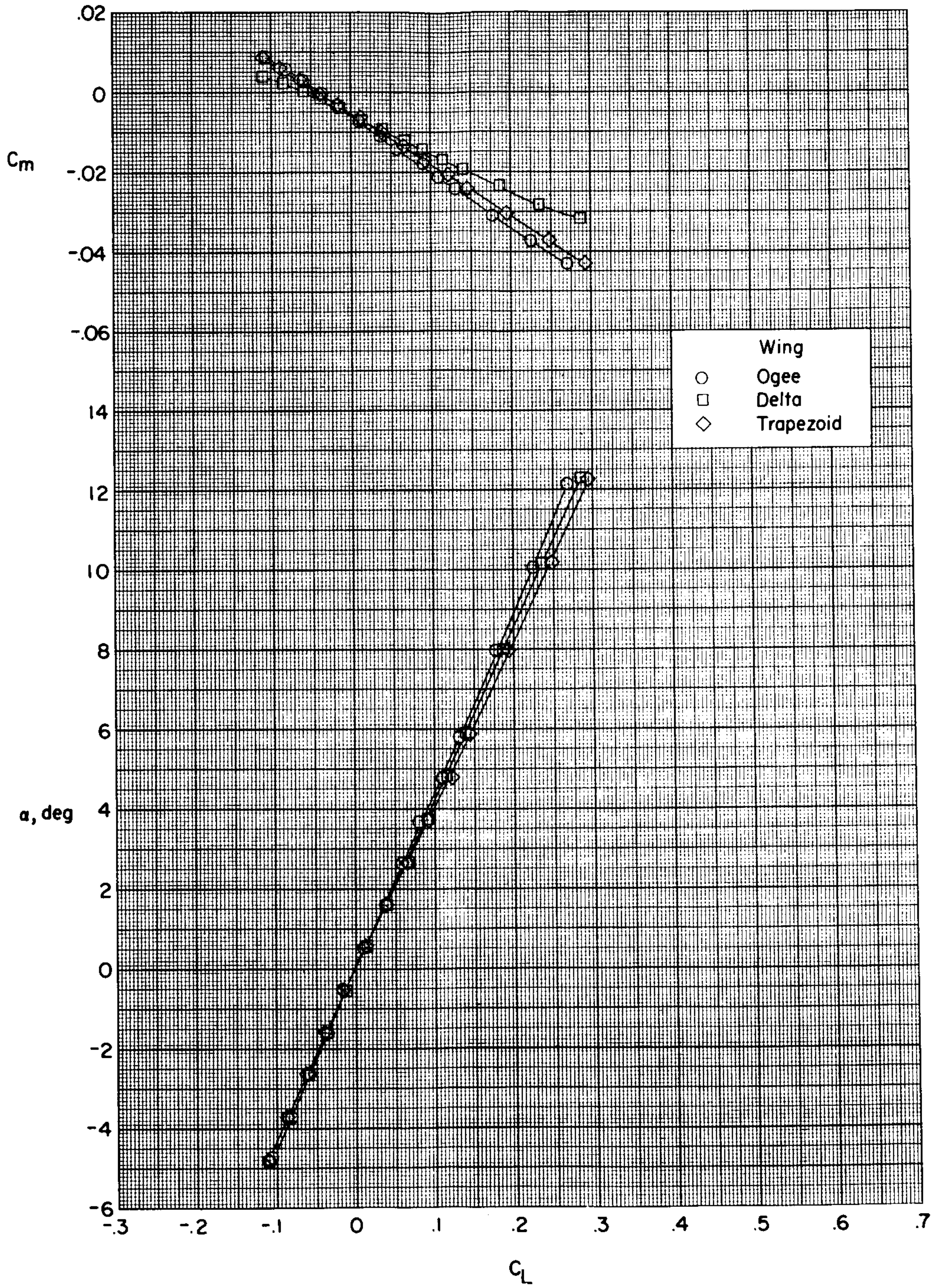

(b) M = 2.86.

Figure 6.- Continued.

[redacted]

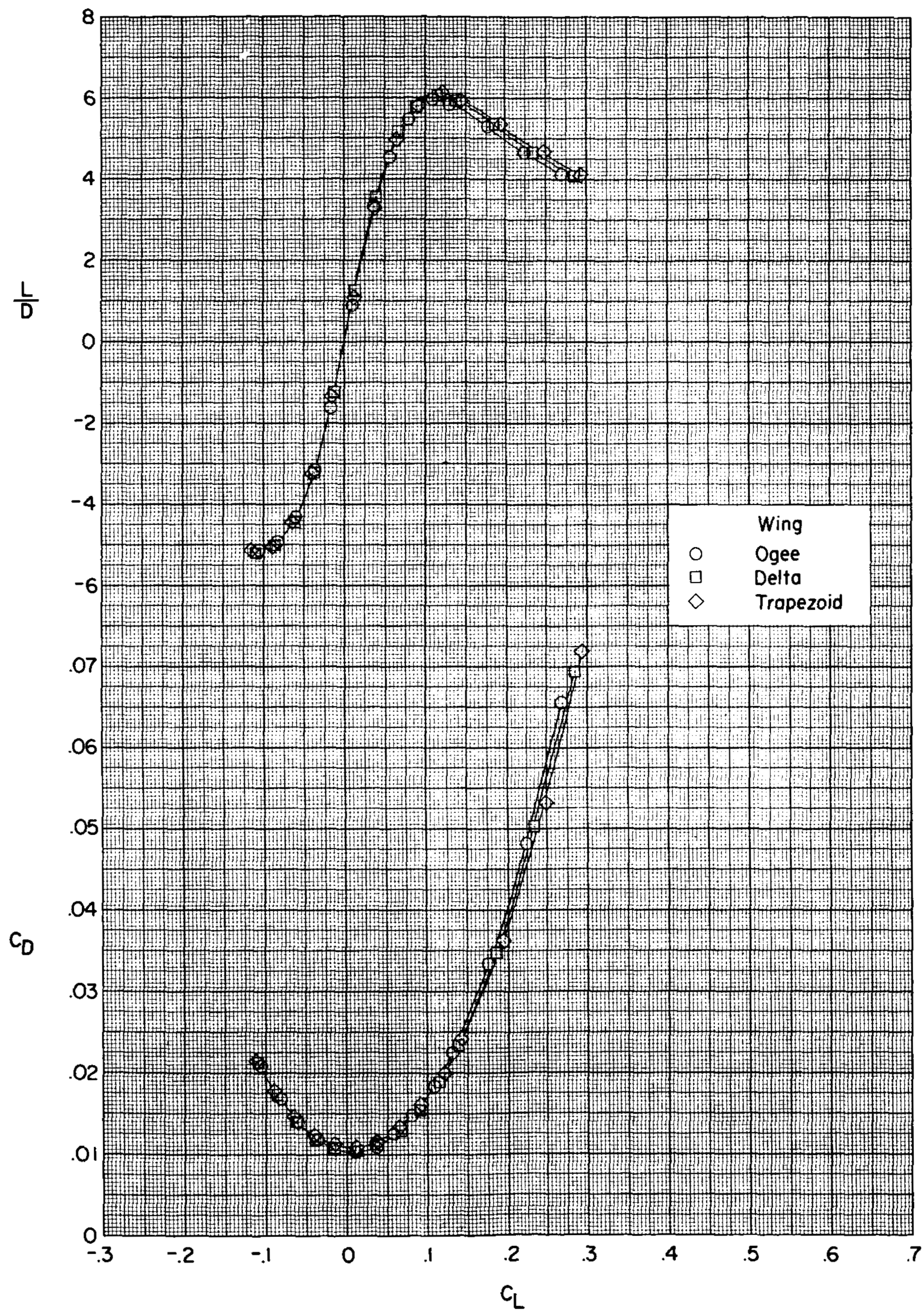

(b) Concluded.

Figure 6.- Concluded.

[redacted]

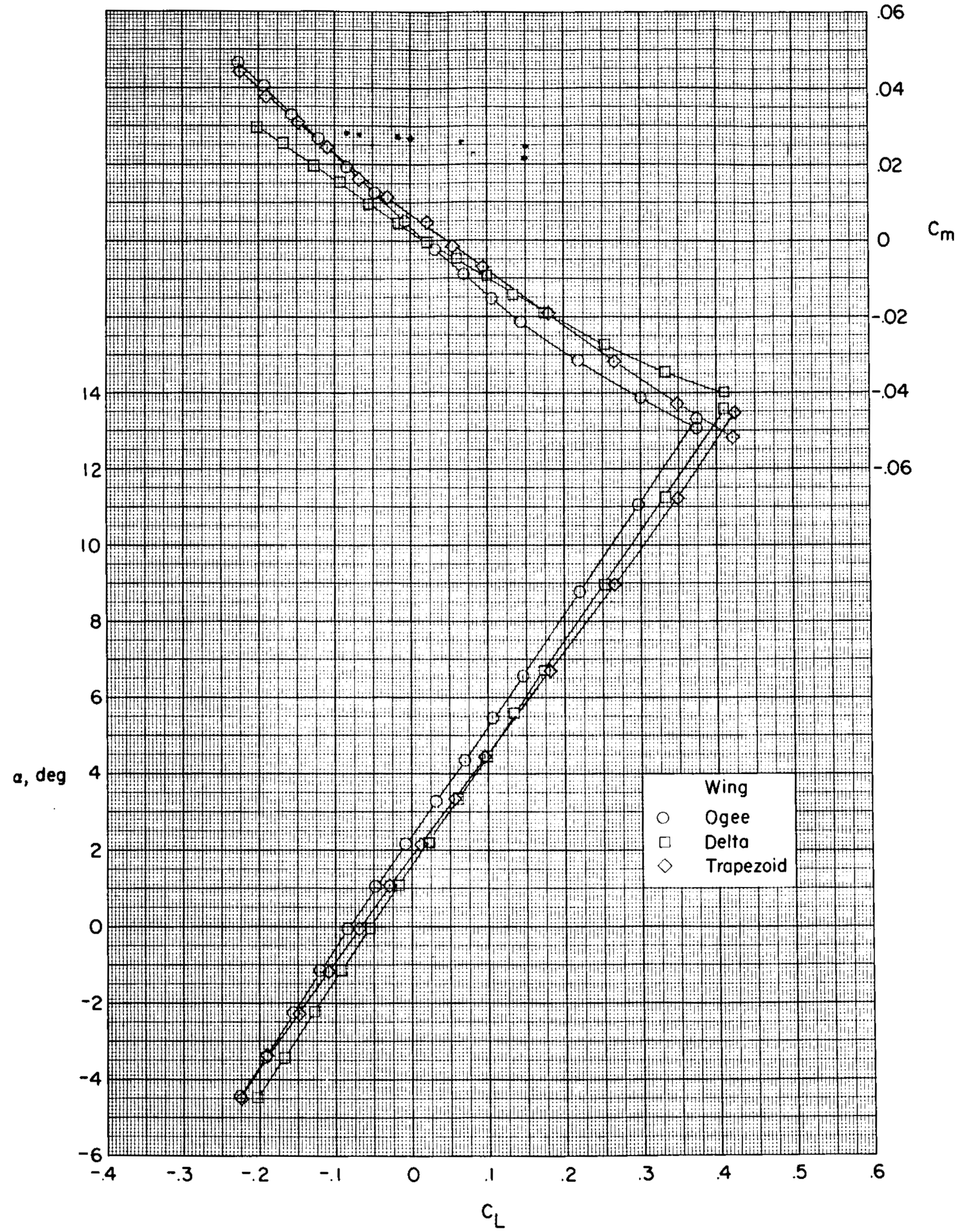

(a) M = 1.80.

Figure 7.- Effect of wing planform on aerodynamic characteristics in pitch. $C_{L,design} = 0.10$; nacelles off.

[redacted]

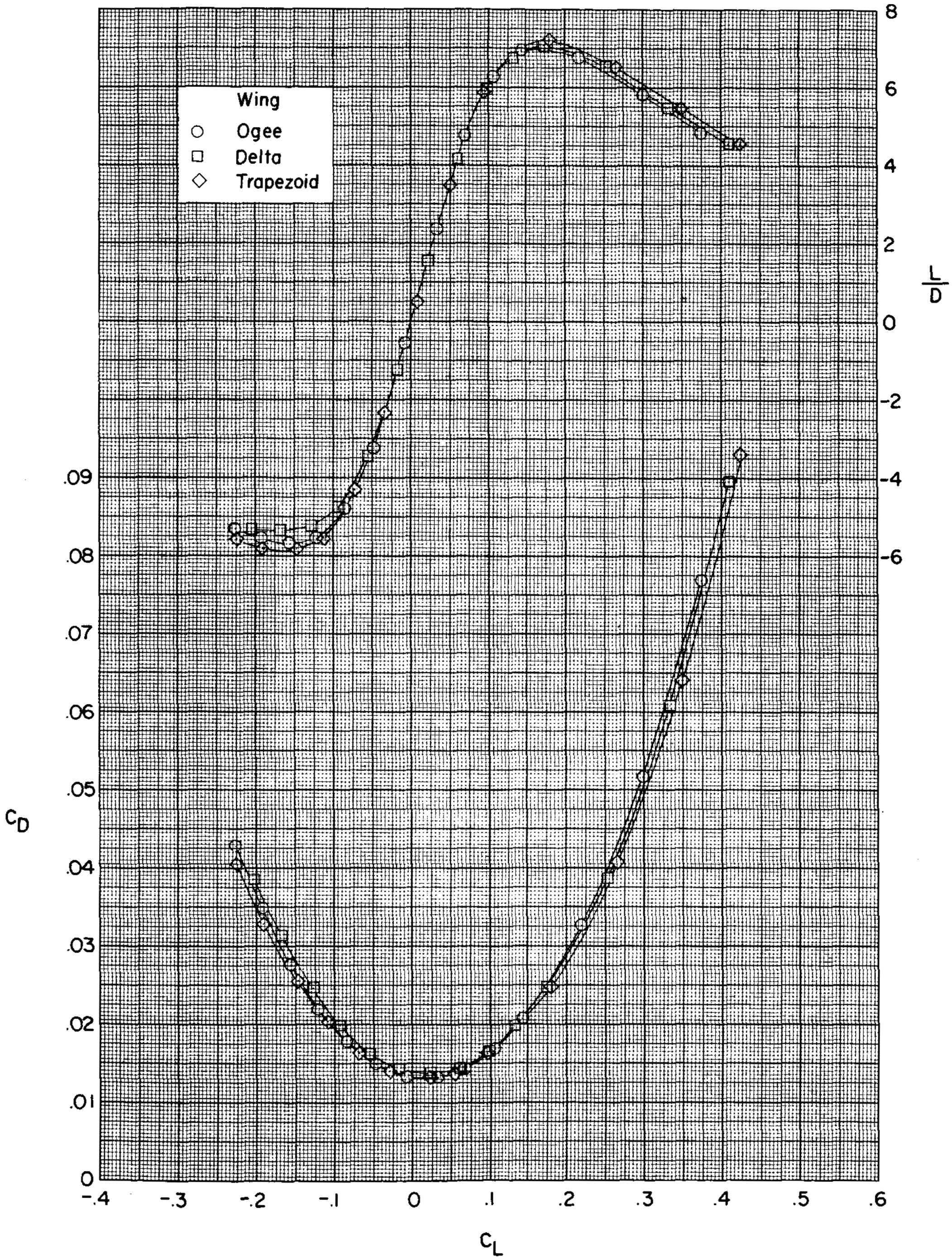

(a) Concluded.

Figure 7.- Continued.

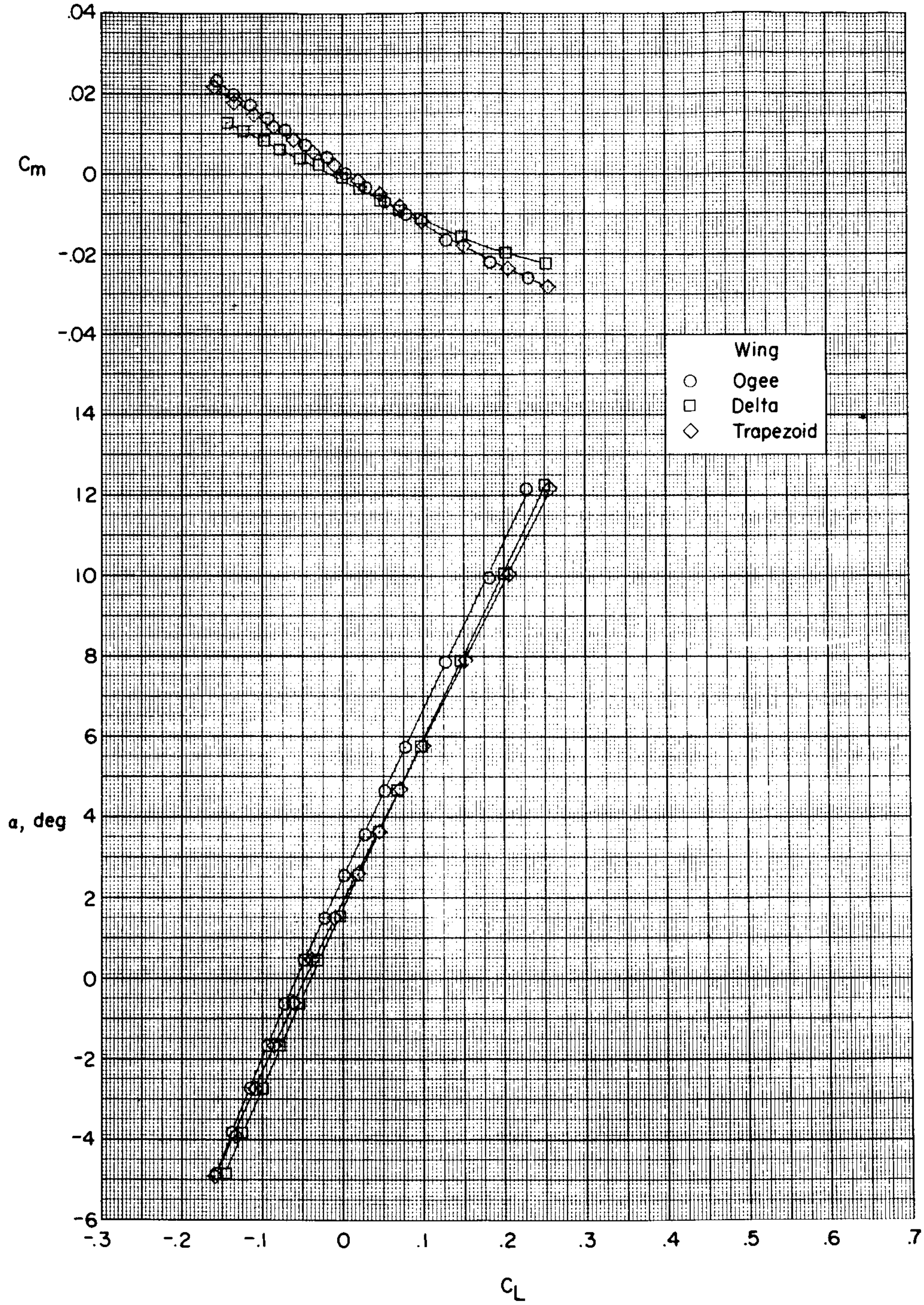

(b) M = 2.86.

Figure 7.- Continued.

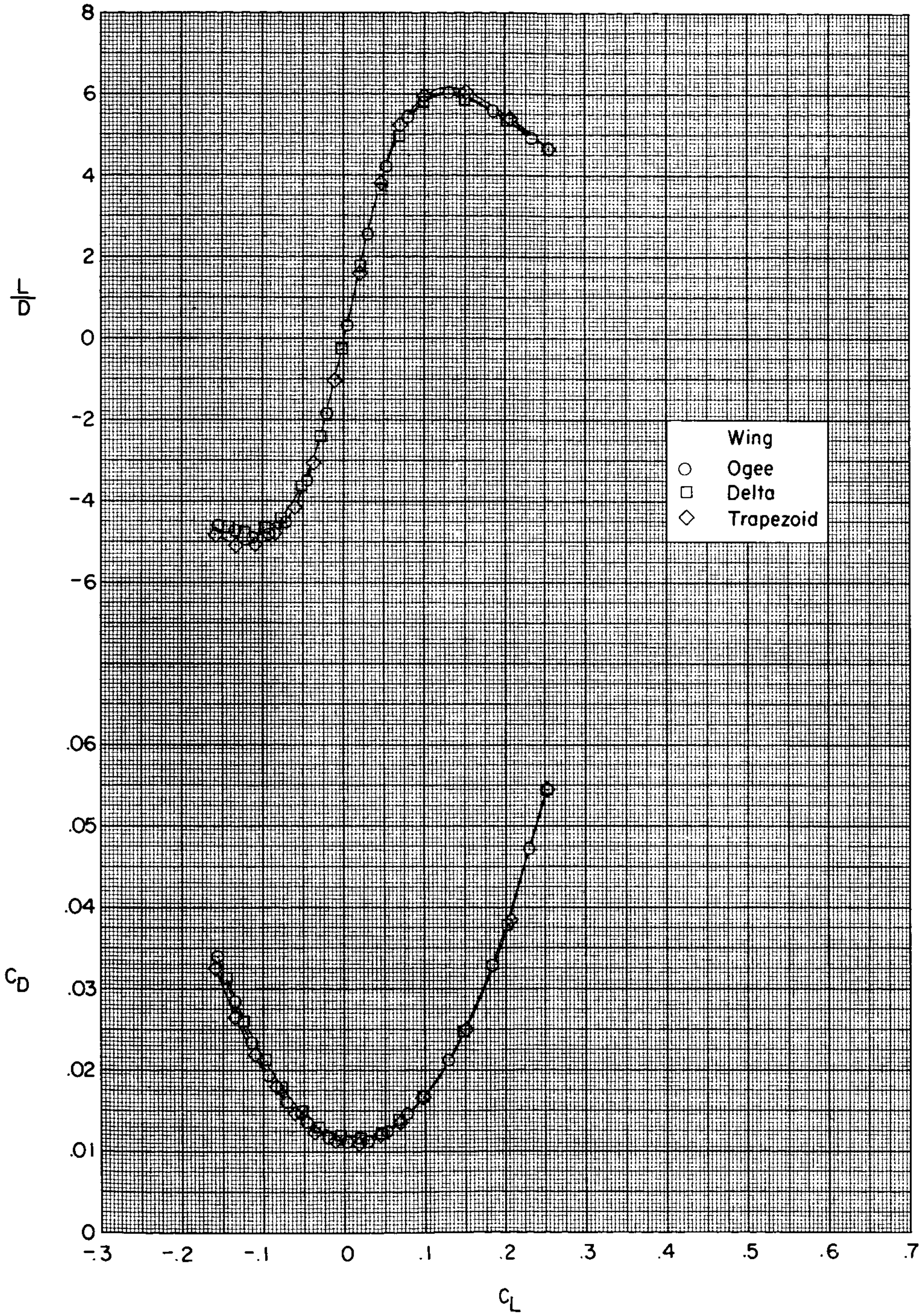

(b) Concluded.

Figure 7.- Concluded.

[redacted]

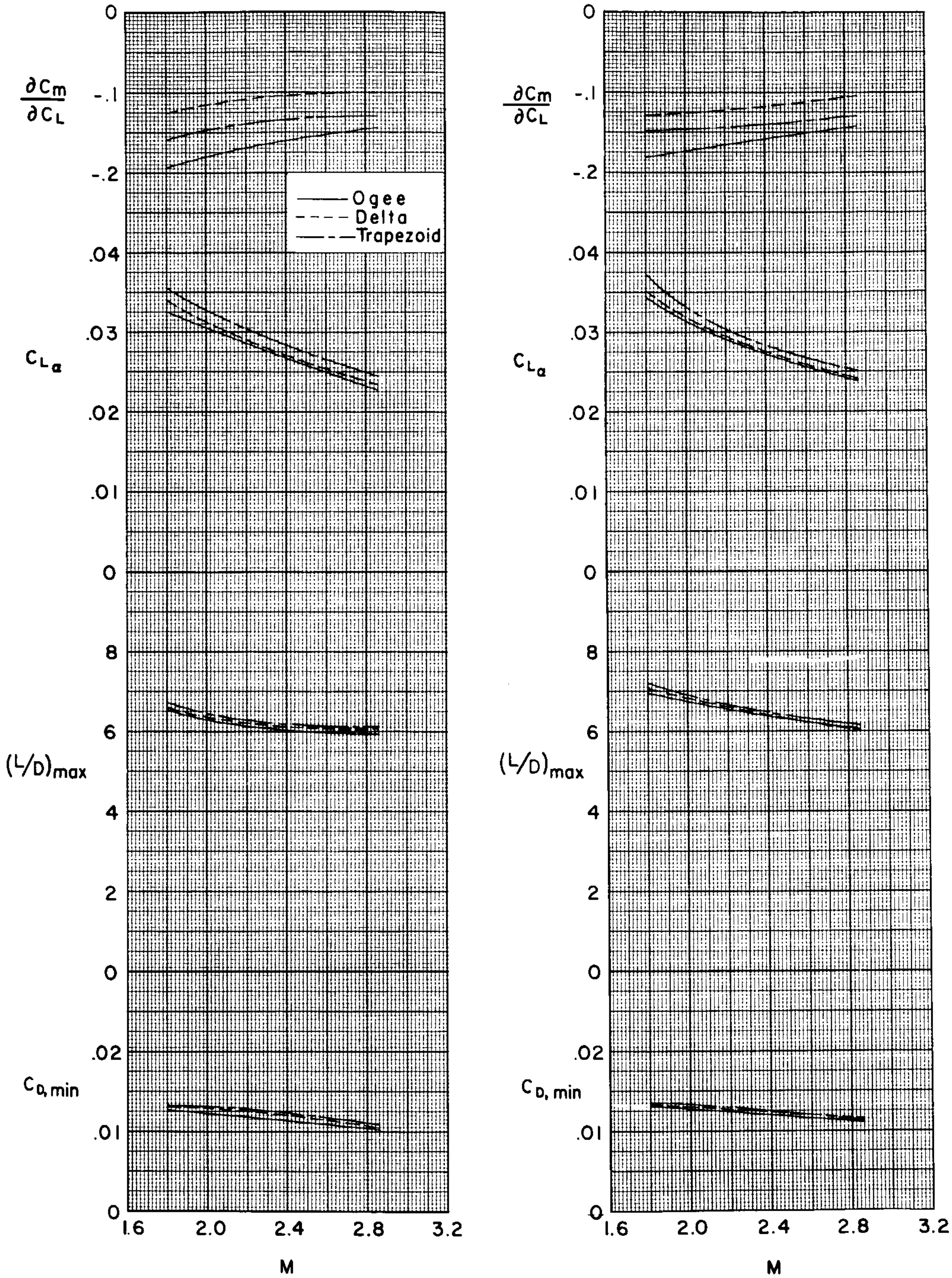

(a) $C_{L,design} = 0$.

(b) $C_{L,design} = 0.10$.

Figure 8.- Variation of longitudinal parameters with Mach number. F_1, nacelles off.

[redacted]

[redacted]

DECLASSIFIED

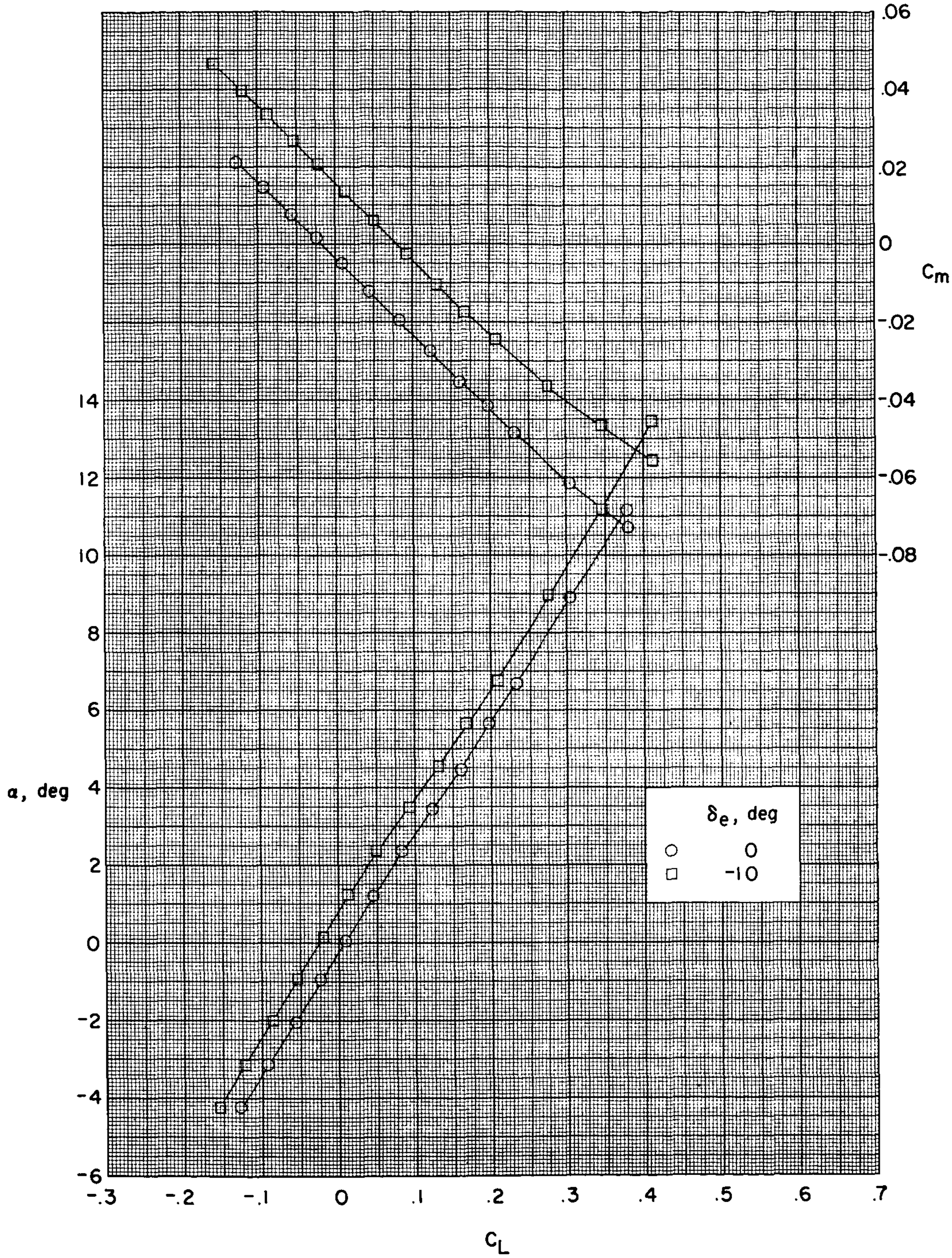

(a) M = 1.80.

Figure 9.- Effect of elevon deflection on aerodynamic characteristics in pitch. Ogee wing; $C_{L,design} = 0$; nacelles on.

[redacted]

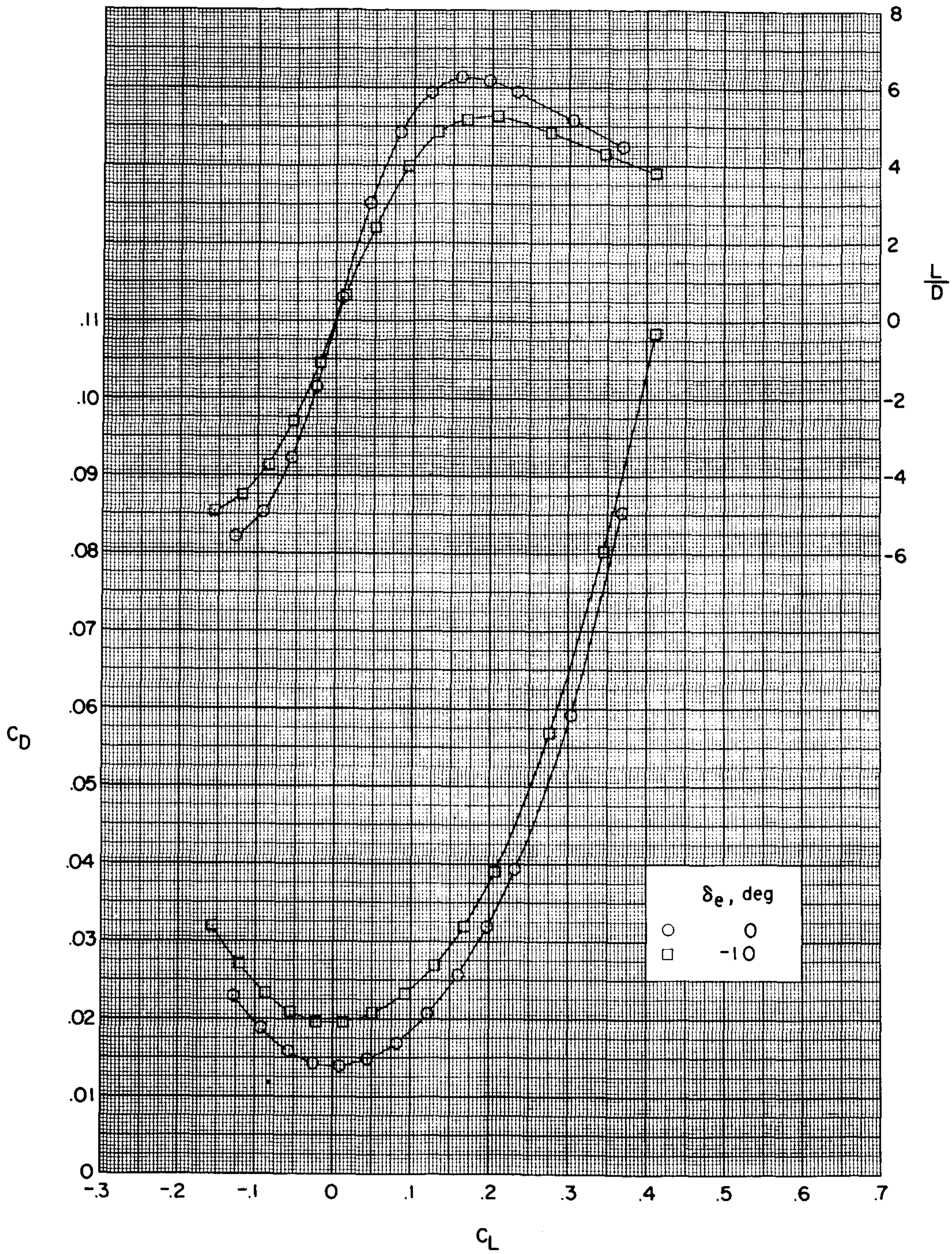

(a) Concluded.

Figure 9.- Continued.

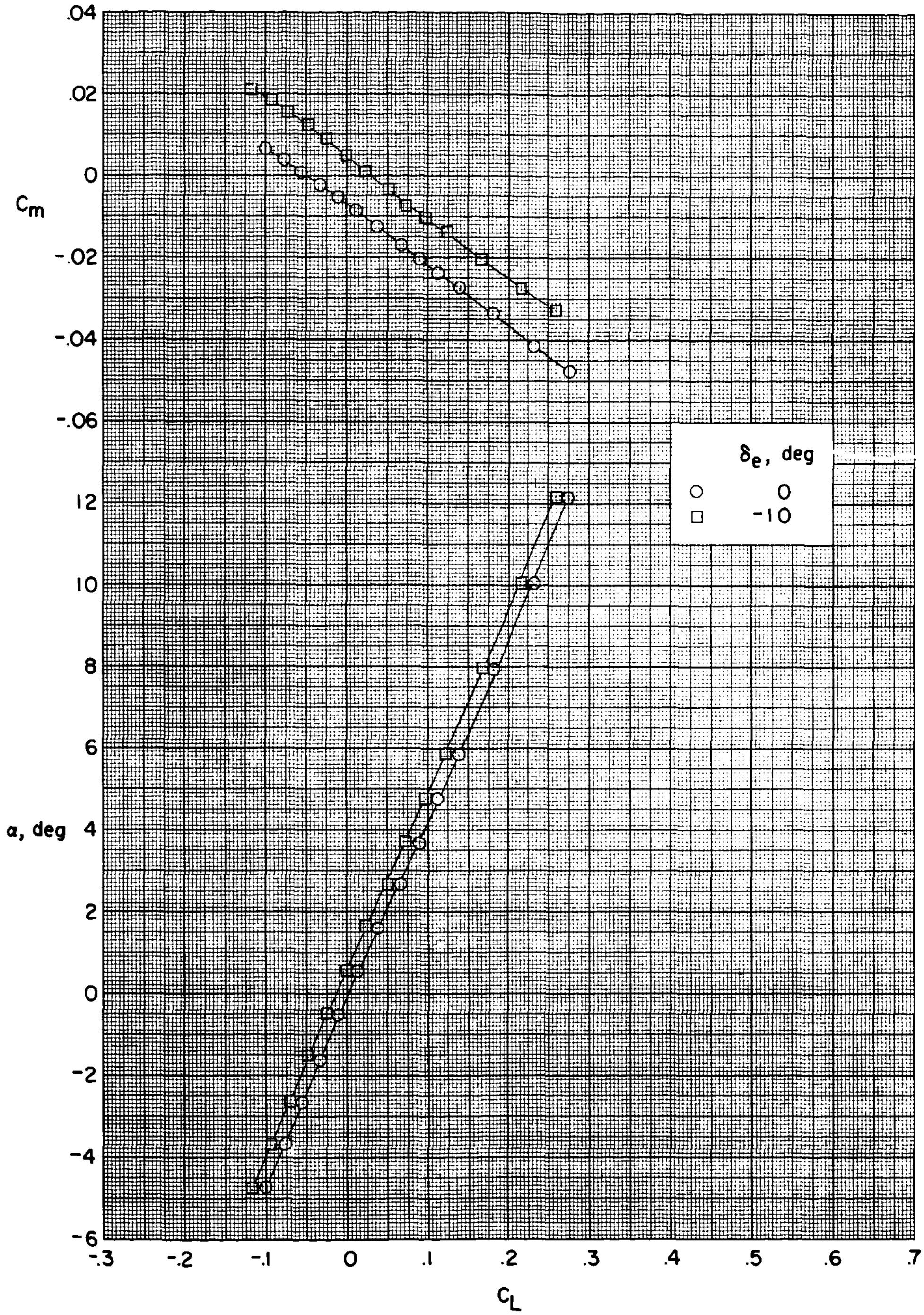

(b) M = 2.86.

Figure 9.- Continued.

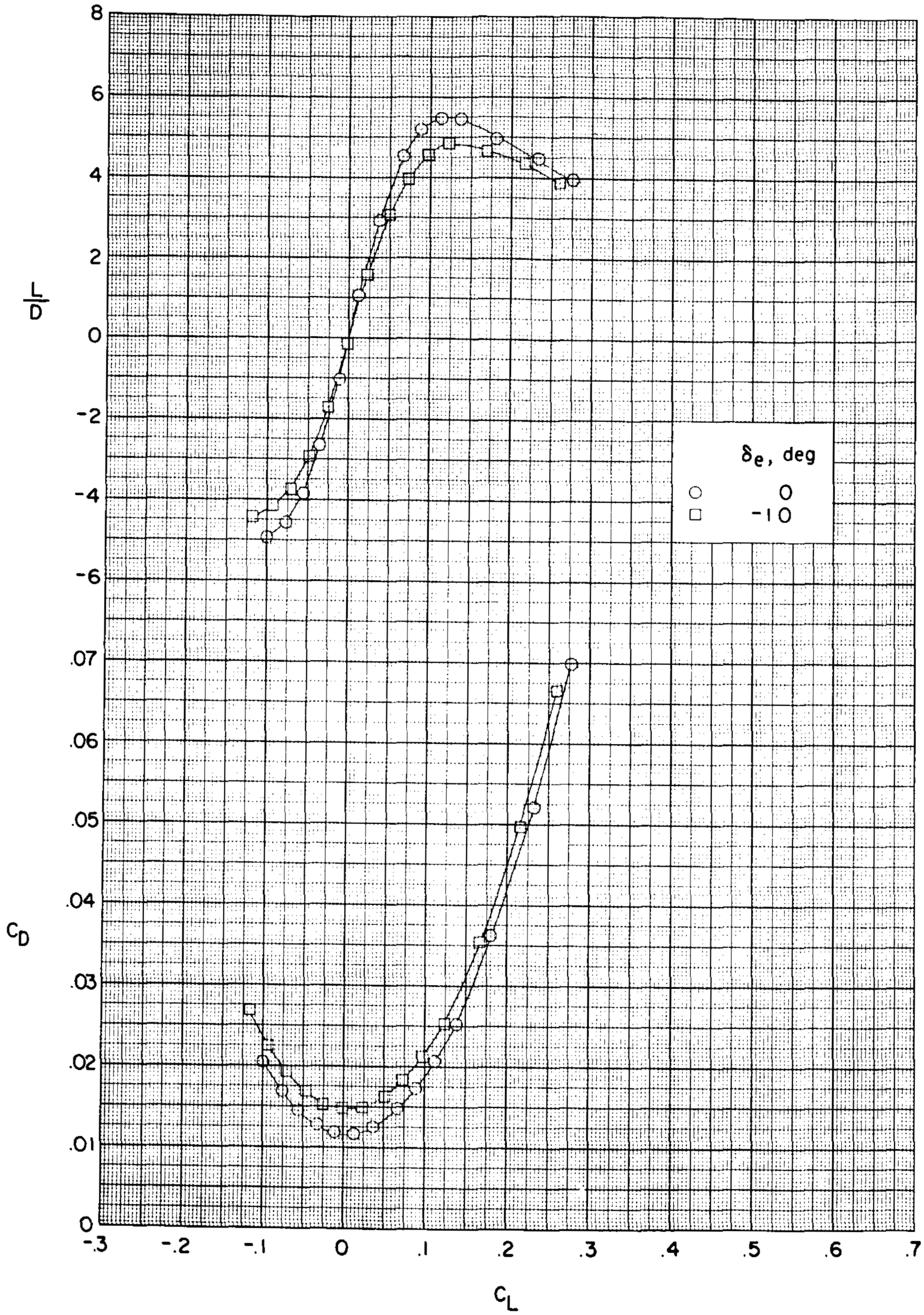

(b) Concluded.

Figure 9.- Concluded.

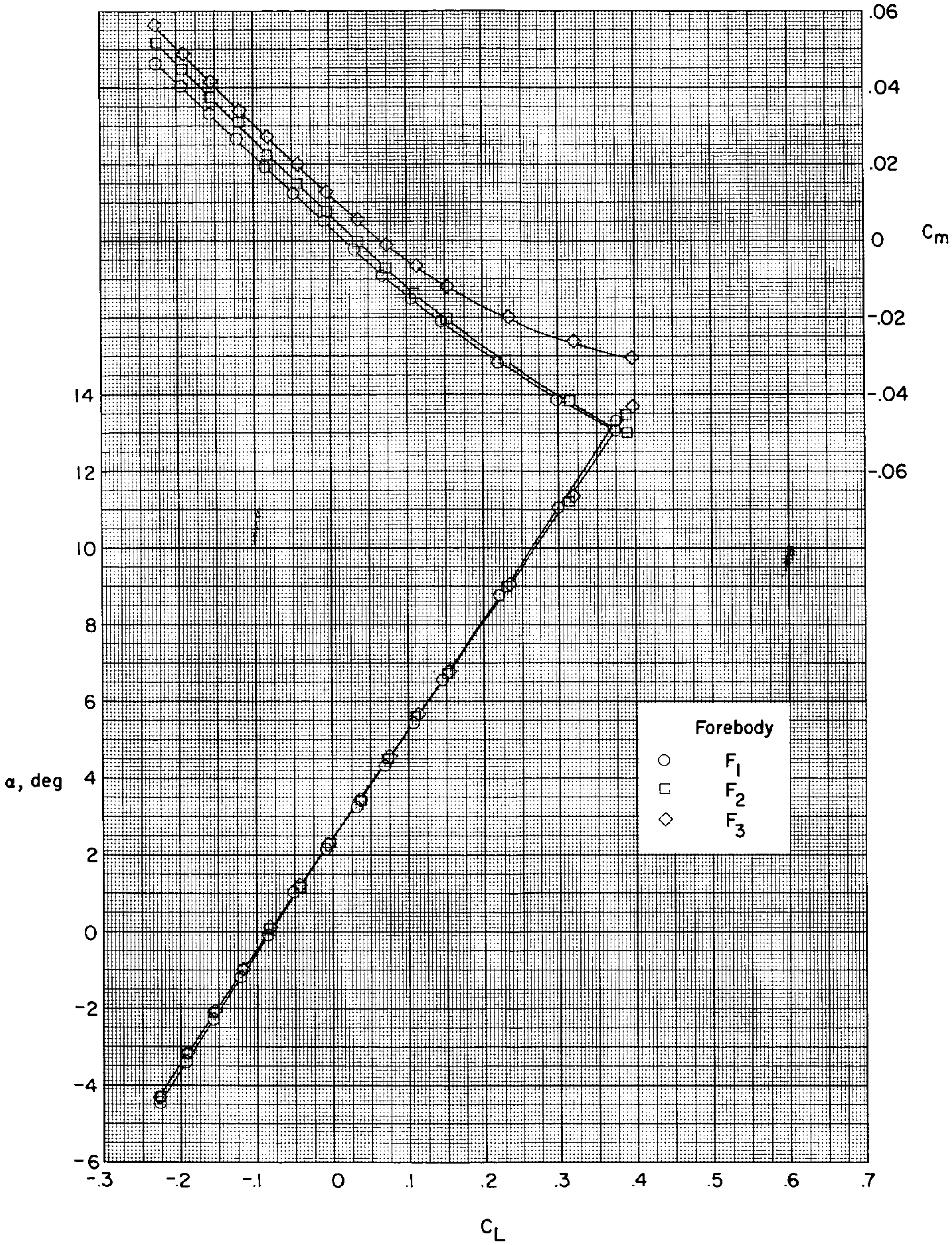

(a) M = 1.80.

Figure 10.- Effect of forebody modification on aerodynamic characteristics in pitch. Ogee wing; $C_{L,design}$ = 0.10; nacelles off.

[redacted]

[redacted]

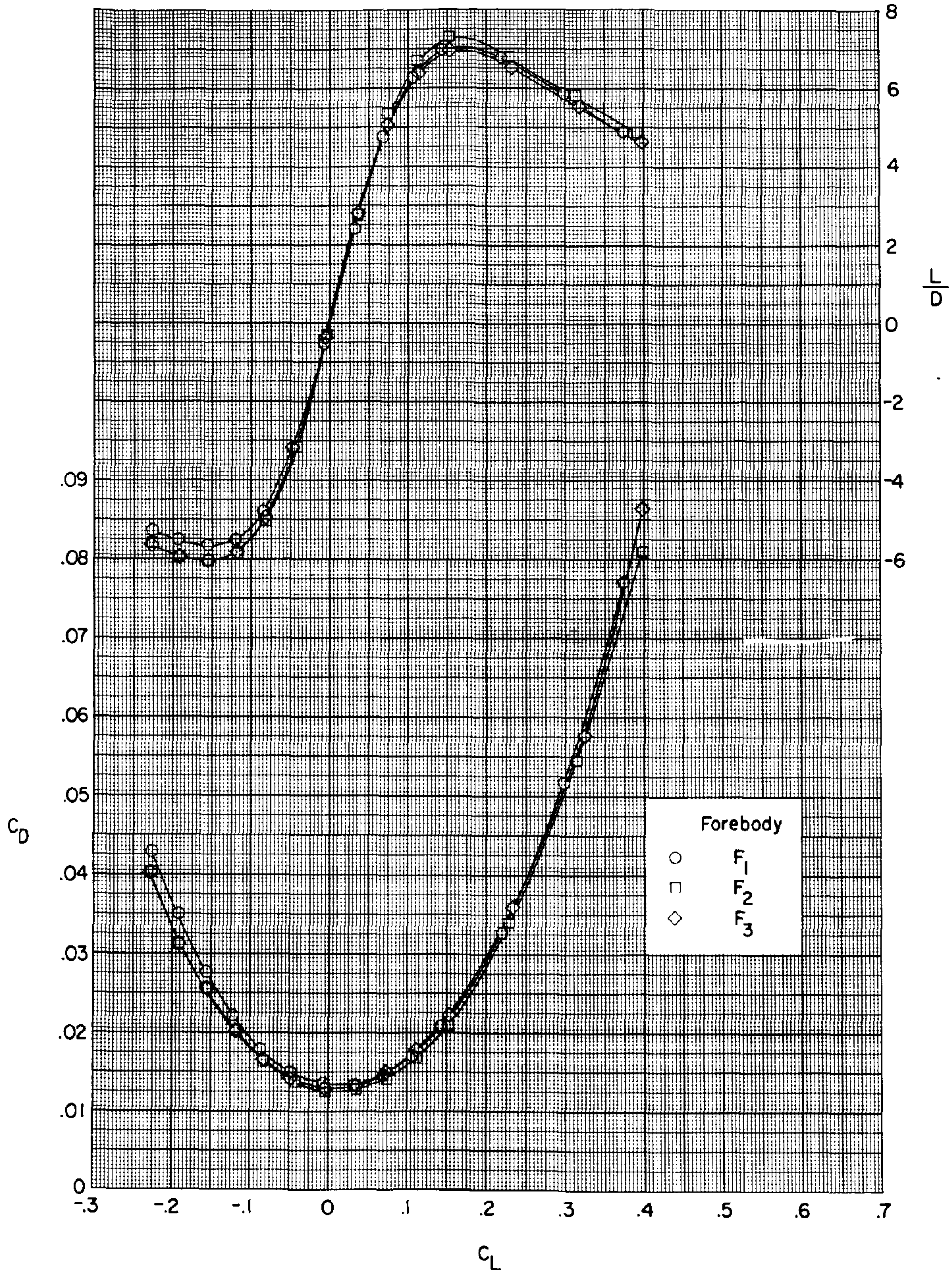

(a) Concluded.

Figure 10.- Continued.

[redacted]

[redacted]

DECLASSIFIED

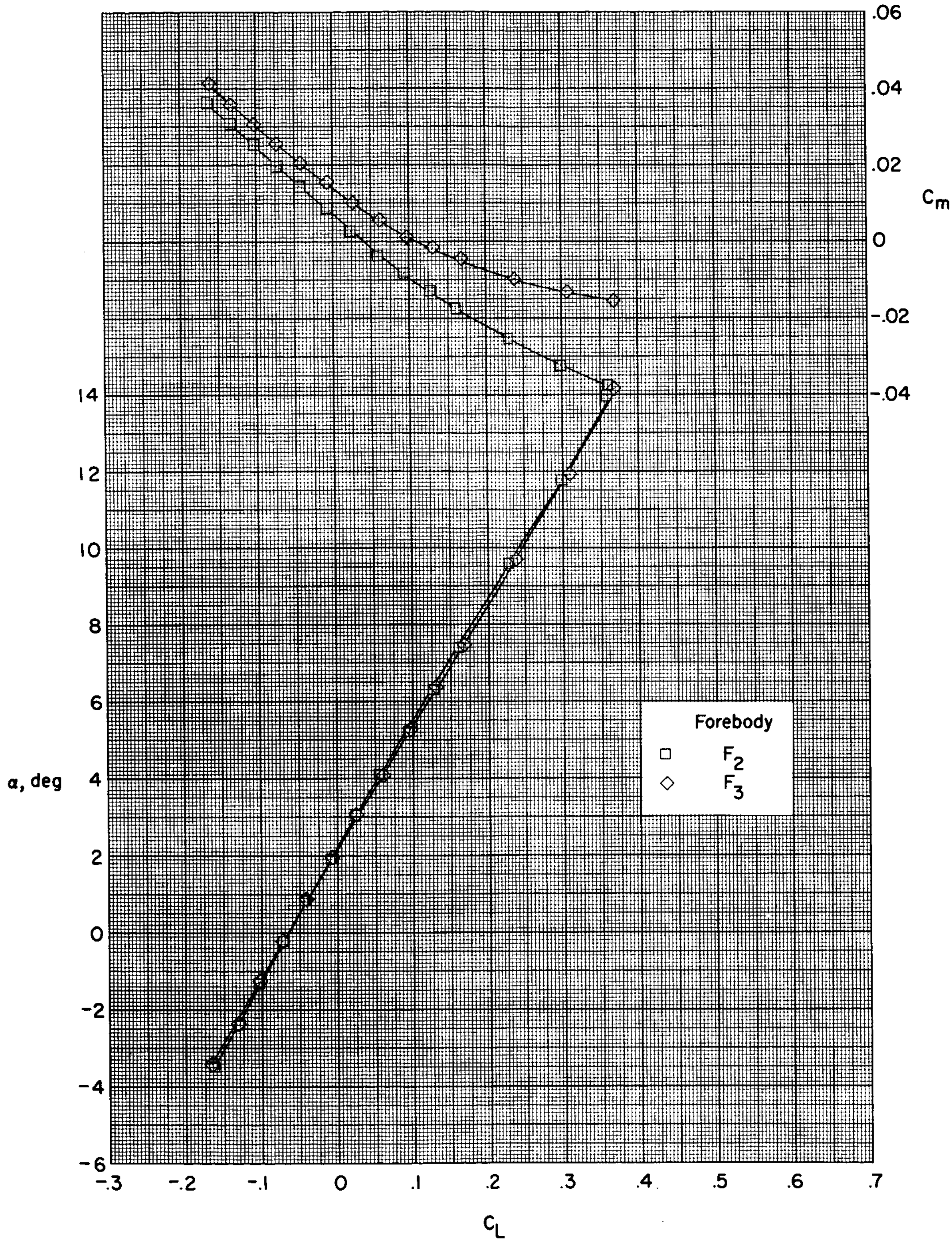

(b) M = 2.20.

Figure 10.- Continued.

[redacted]

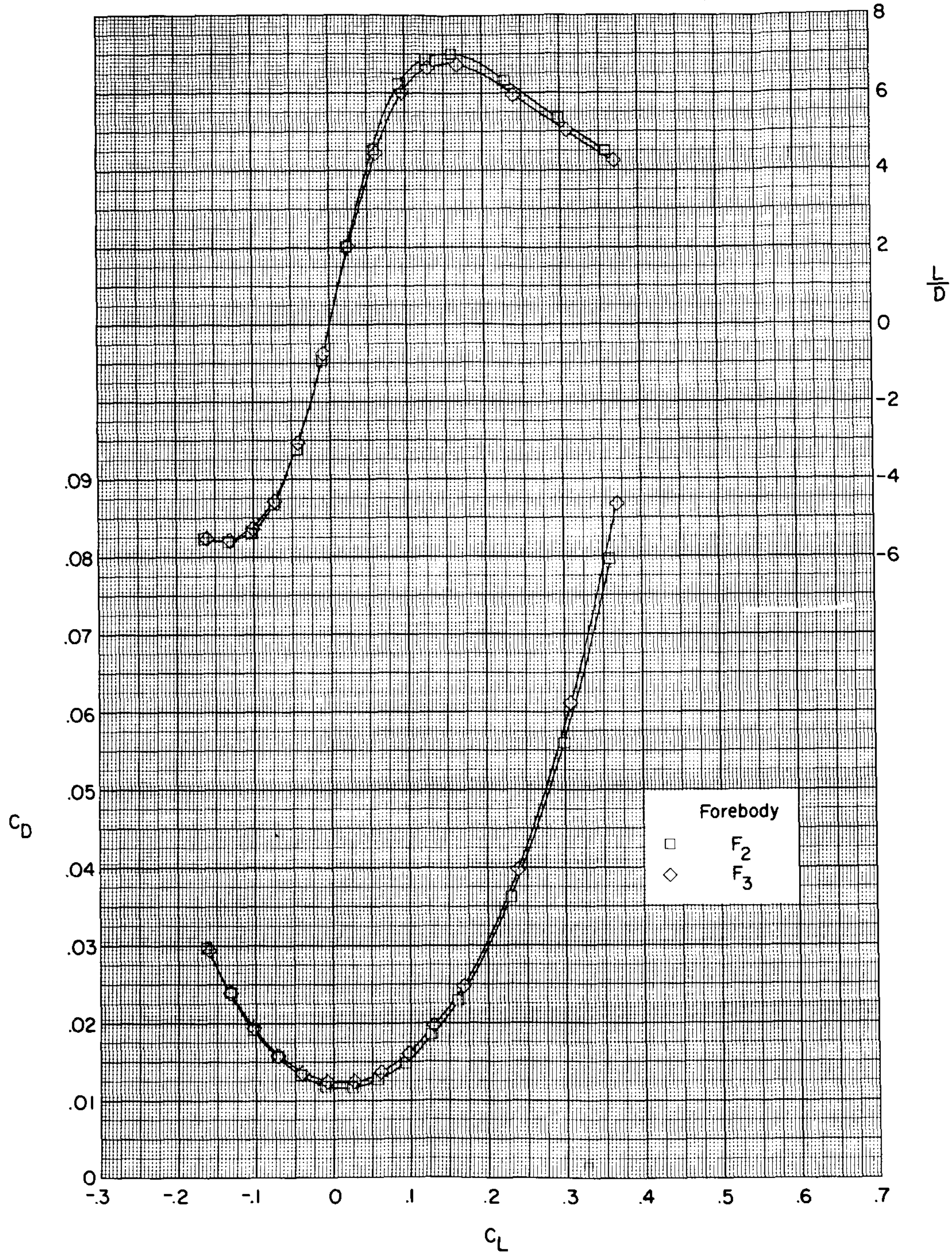

(b) Concluded.

Figure 10.- Continued.

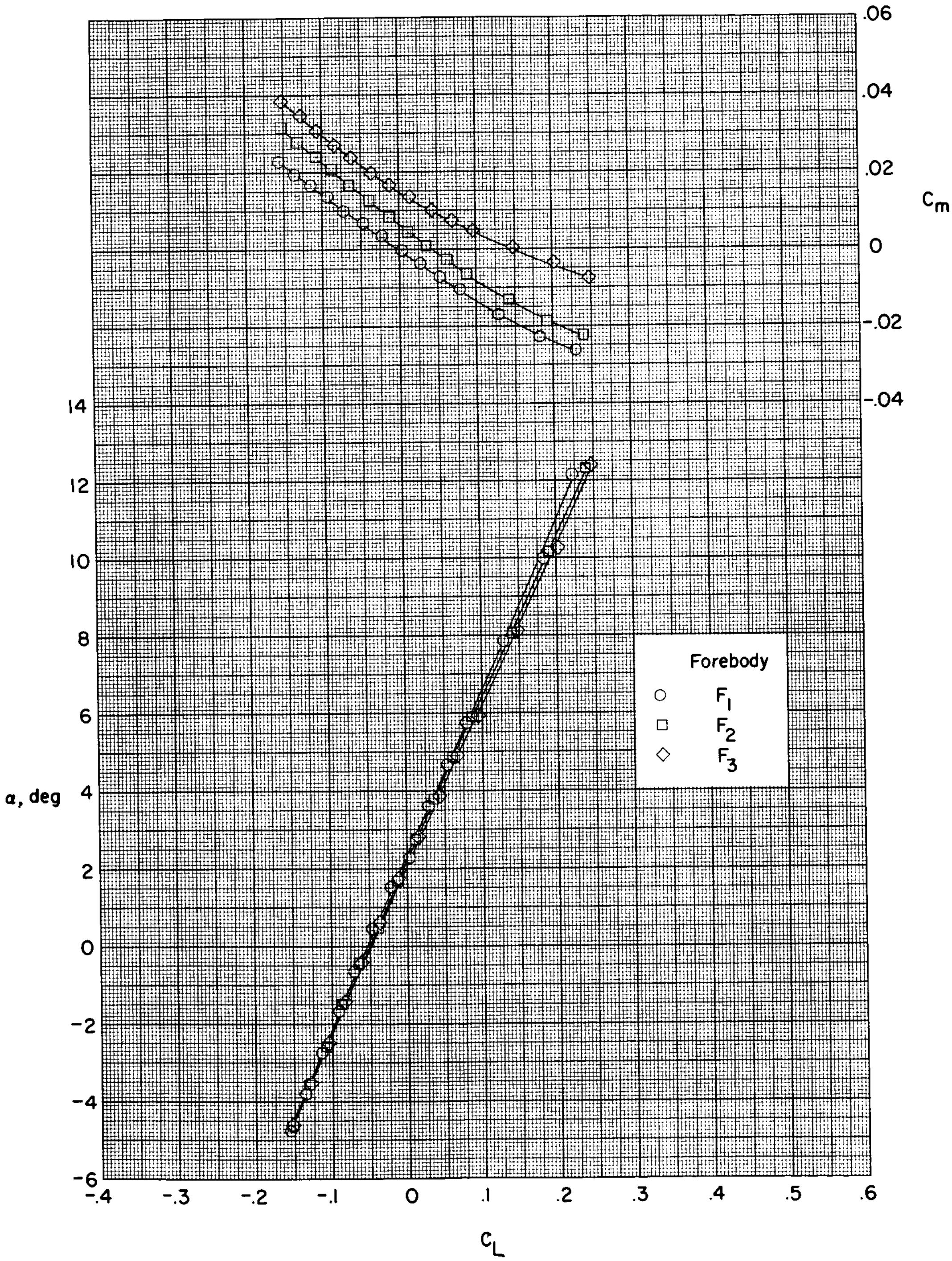

(c) M = 2.86.

Figure 10.- Continued.

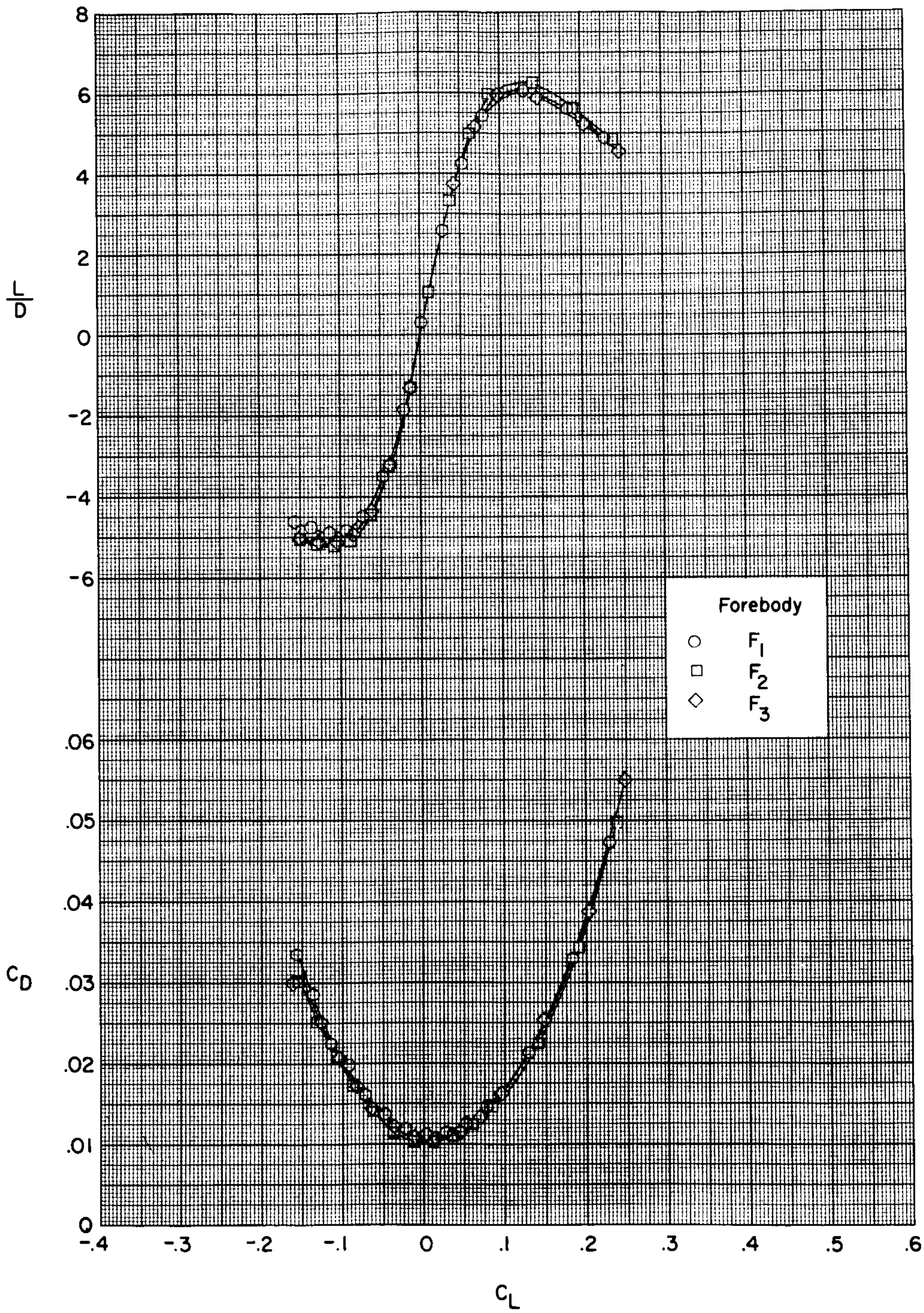

(c) Concluded.

Figure 10.- Concluded.

[redacted]

DECLASSIFIED

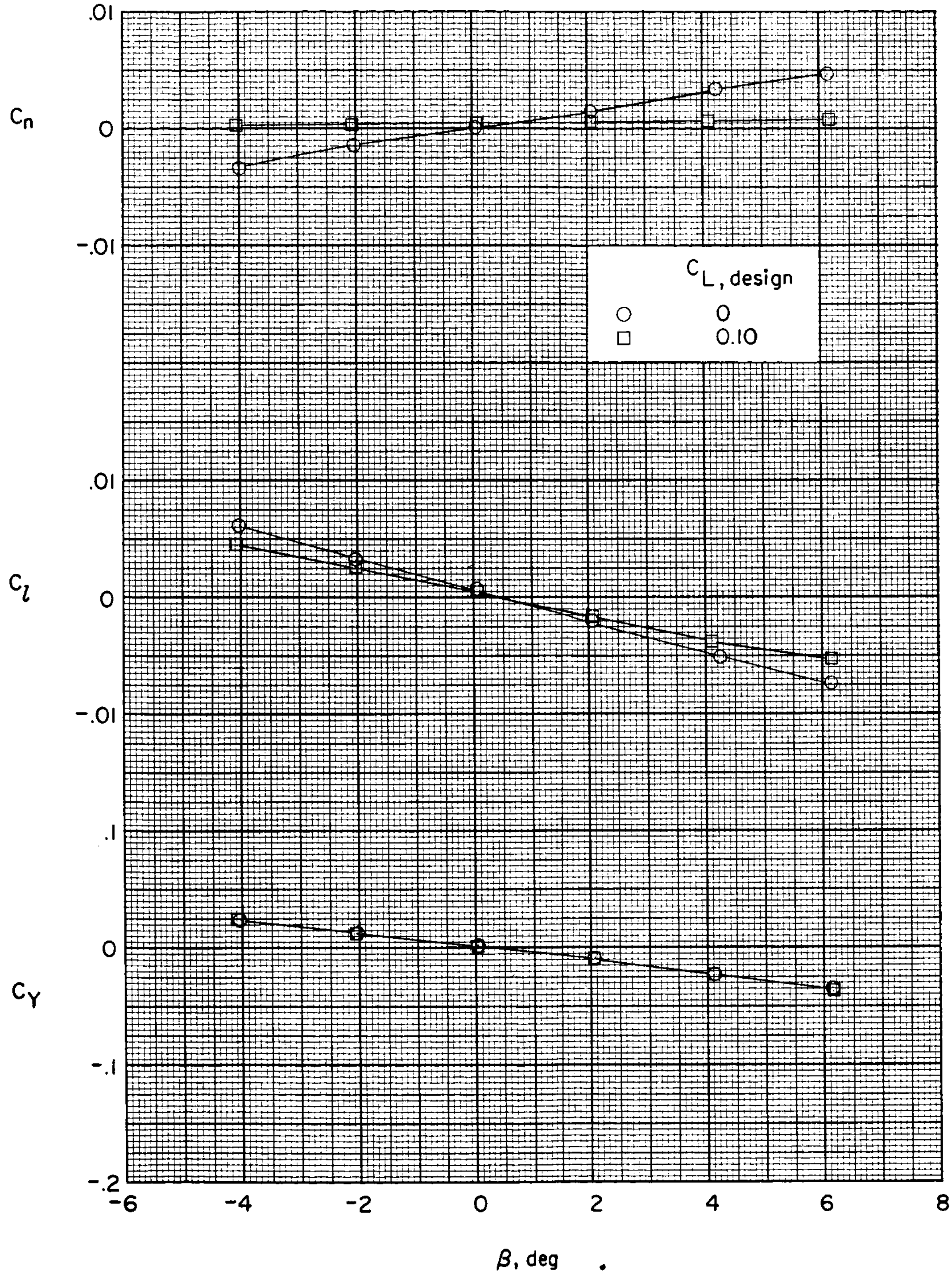

(a) M = 1.80.

Figure 11.- Effect of wing camber and twist on aerodynamic characteristics in sideslip. Ogee wing; nacelles off; $\alpha = 8^{\circ}$.

[redacted]

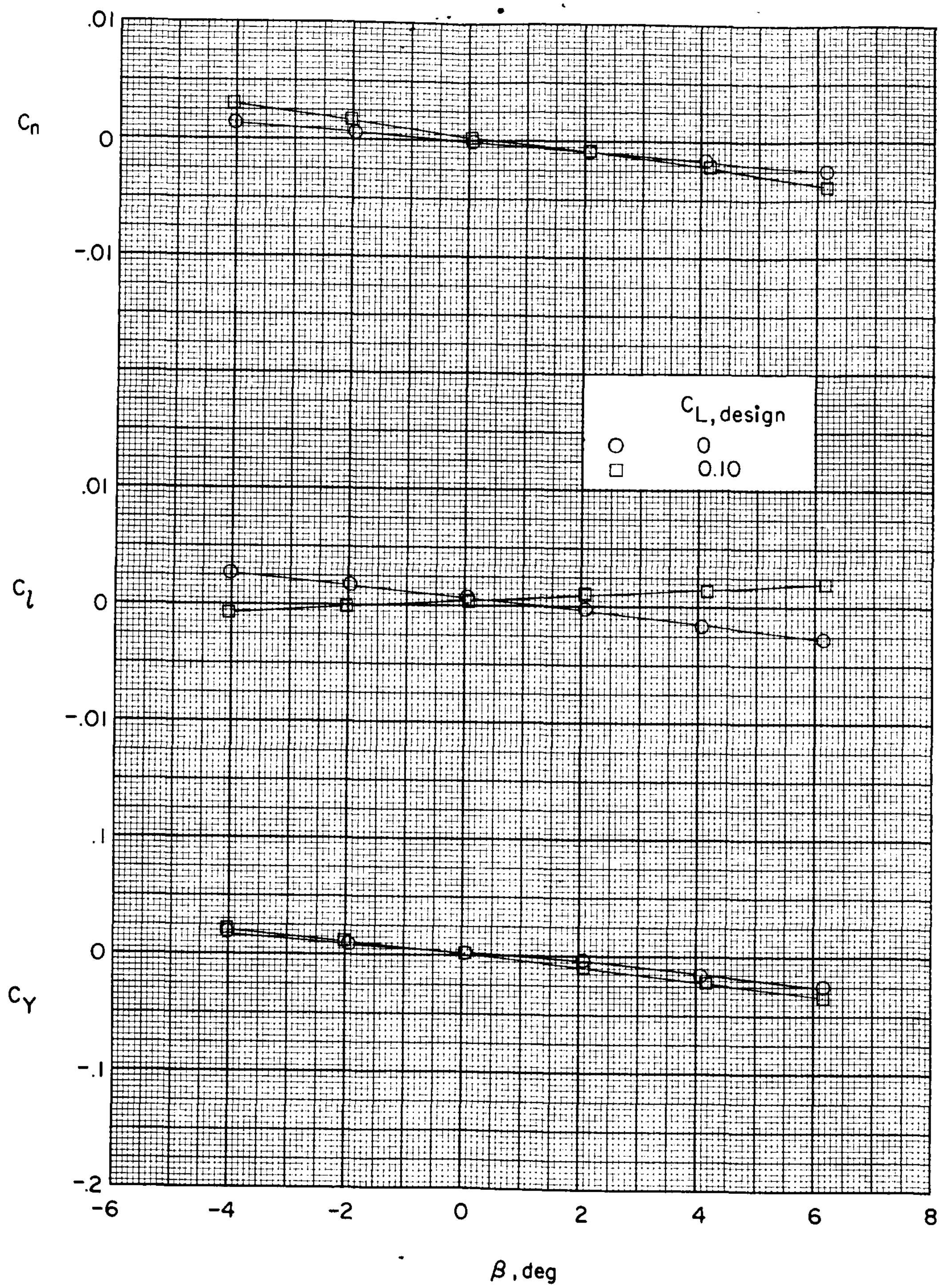

(b) M = 2.86.

Figure 11.- Concluded.

[redacted]

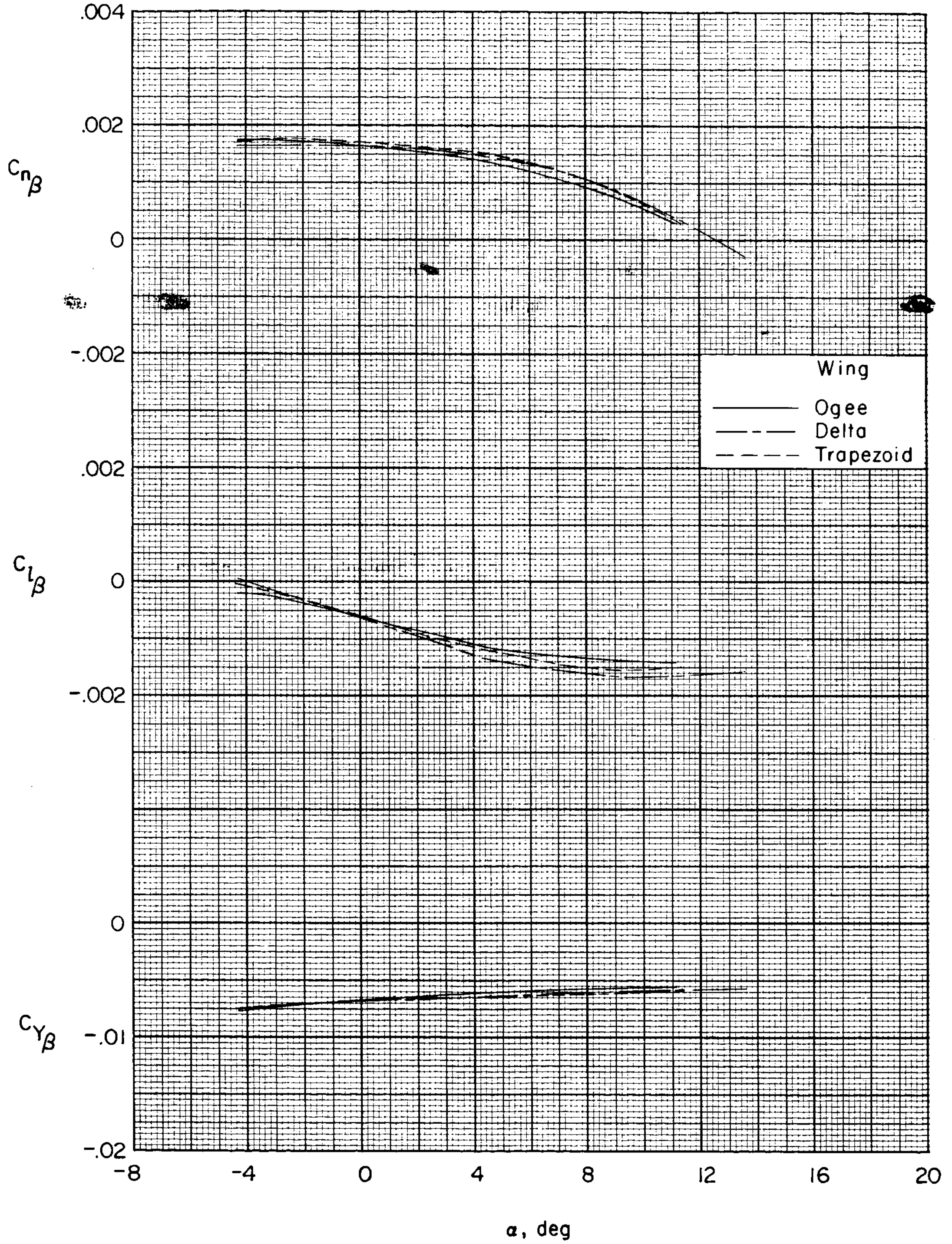

(a) M = 1.80.

Figure 12.- Effect of wing planform on sideslip parameters. $C_{L,design} = 0$; nacelles off.

[redacted]

[redacted]

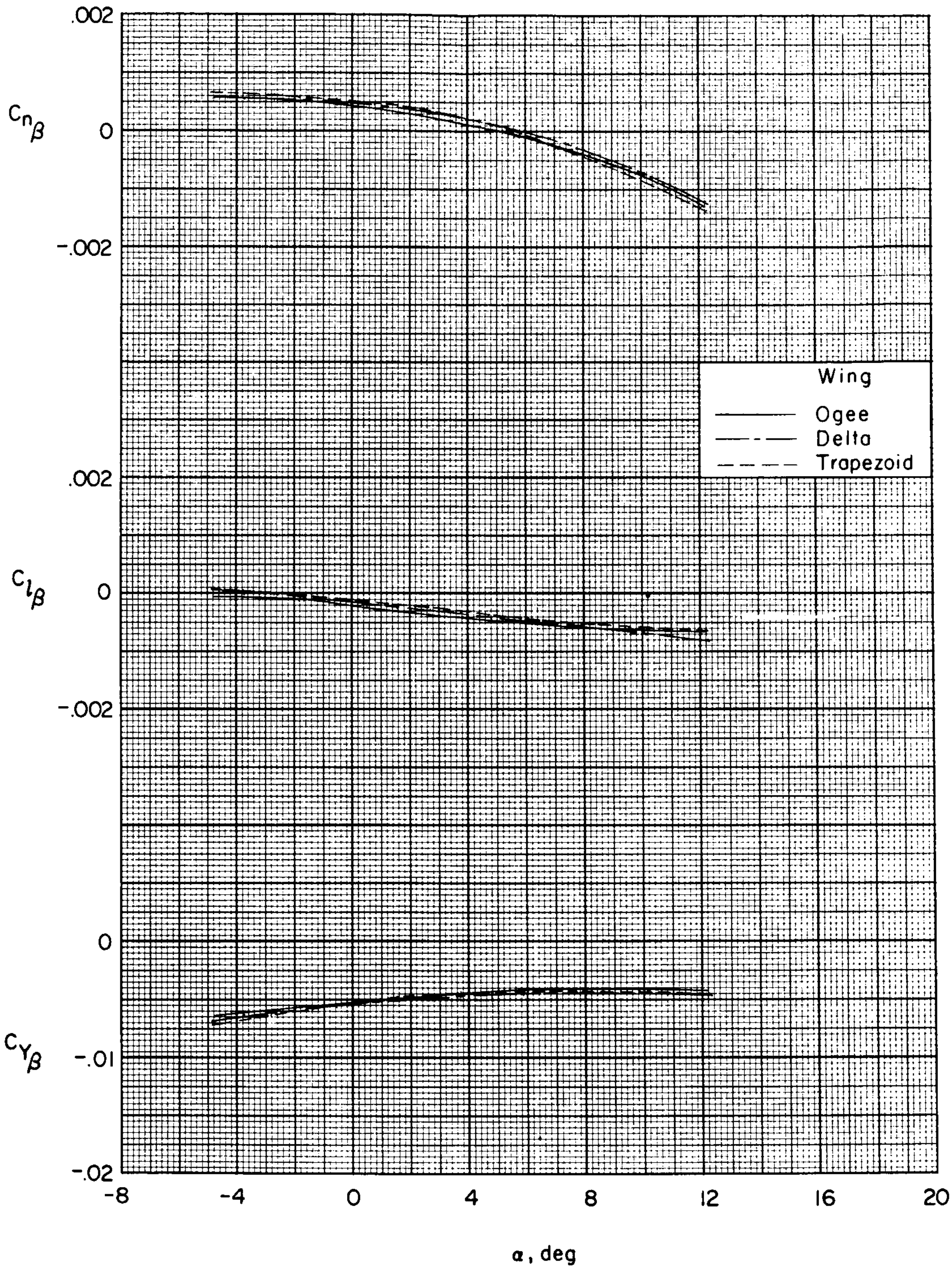

(b) M = 2.86.

Figure 12.- Concluded.

[redacted]

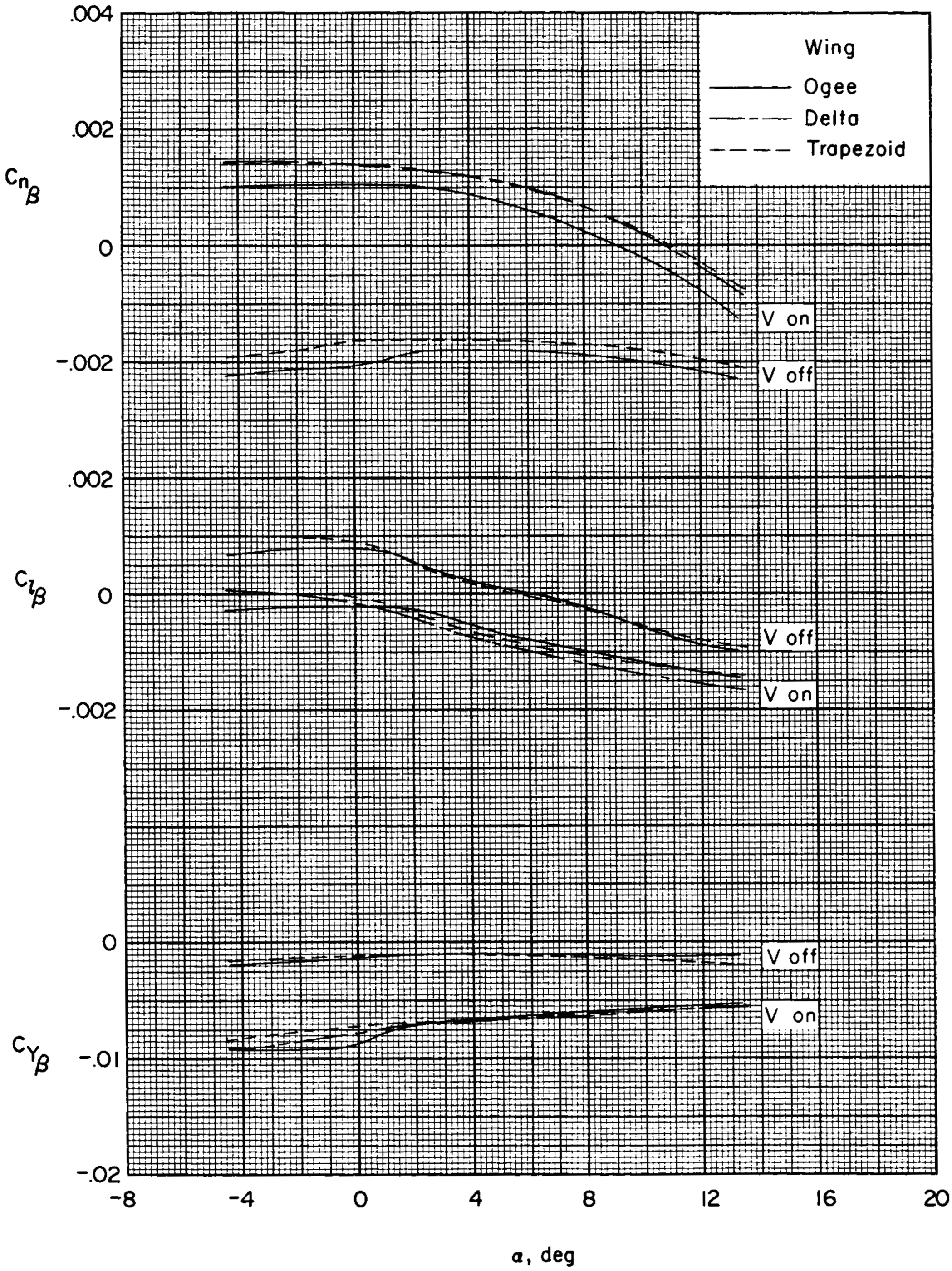

(a) M = 1.80.

Figure 13.- Effect of wing planform and vertical tail (V) on sideslip parameters. $C_{L,design}$ = 0.10; nacelles off.

[redacted]

[redacted]

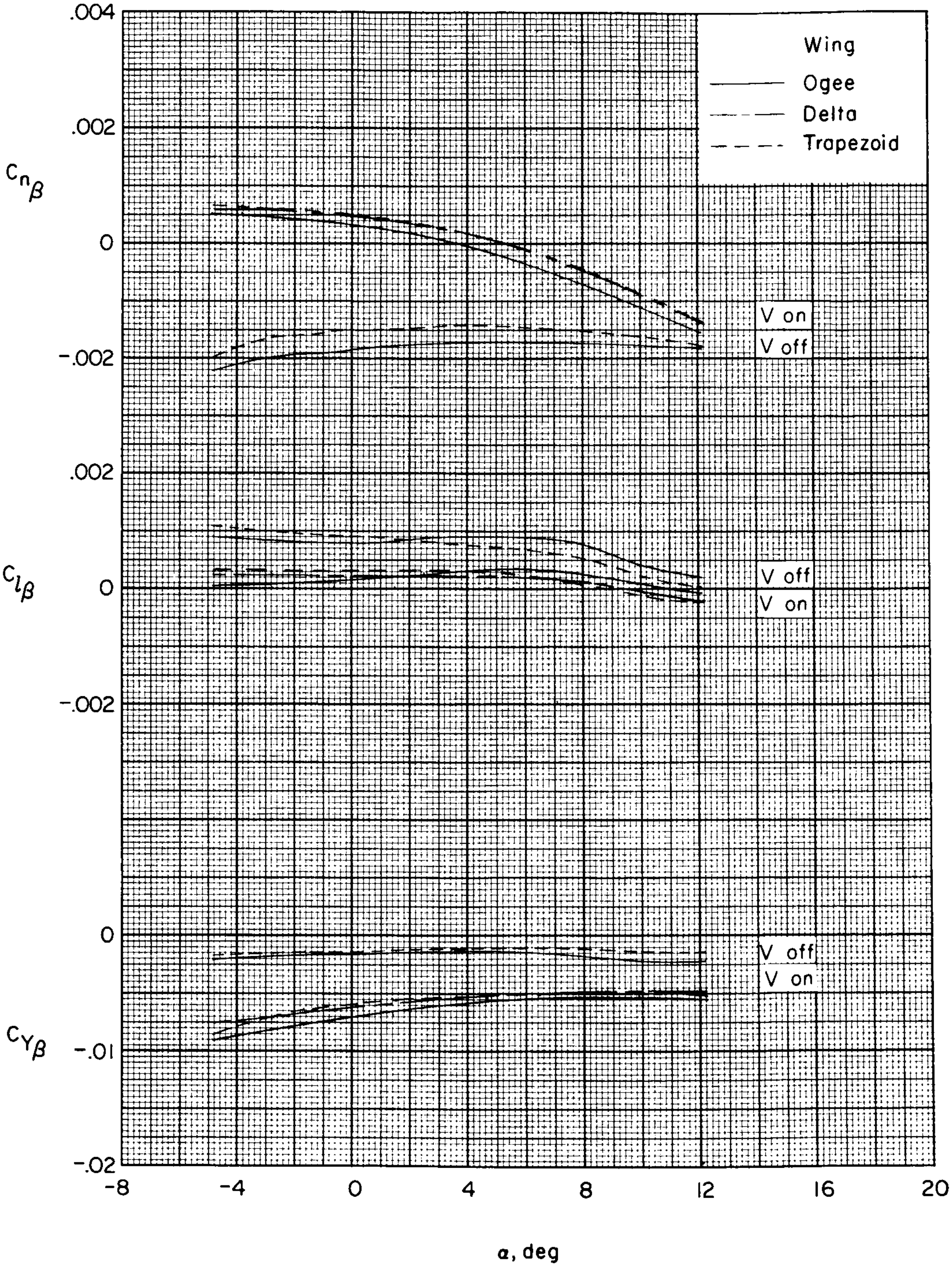

(b) M = 2.86.

Figure 13.- Concluded.

[redacted]

NASA-Langley, 1964 L-3994